Article

Discovery of Orally Bioavailable Chromone Derivatives as Potent and Selective BRD4 Inhibitors: Scaffolding Hopping, Optimization and Pharmacological Evaluation

Zhiqing Liu, Haiying Chen, Pingyuan Wang, Yi Li, Eric A. Wold, Paul G. Leonard, Sarah Joseph, Allan R. Brasier, Bing Tian, and Jia Zhou

Just Accepted

Discovery of Orally Bioavailable Chromone Derivatives as Potent and Selective BRD4 Inhibitors: Scaffolding Hopping, Optimization and Pharmacological Evaluation

Zhiqing Liu,[†] Haiying Chen,[†] Pingyuan Wang,[†] Yi Li,[†] Eric A. Wold,[†] Paul G. Leonard,[£] Sarah Joseph,[£] Allan R. Brasier,[‖,*] Bing Tian,[‡,§,*] and Jia Zhou[†,§,ξ,*]

[†]Chemical Biology Program, Department of Pharmacology and Toxicology, [‡]Department of Internal Medicine, [§]Sealy Center for Molecular Medicine, [ξ]Institute for Translational Sciences, University of Texas Medical Branch, Galveston, TX 77555, USA

[£]Core for Biomolecular Structure and Function, MD Anderson Cancer Center, 1881 East Road, Houston, TX, 77054, USA

[‖]Institute for Clinical and Translational Research (ICTR), University of Wisconsin-Madison School of Medicine and Public Health, 4248 Health Sciences Learning Center, Madison, WI 53705, USA

Corresponding authors: Dr. Jia Zhou, Chemical Biology Program, Department of Pharmacology and Toxicology, University of Texas Medical Branch, Galveston, Texas 77555, United States. Tel: +1 (409) 772-9748; E-mail: jizhou@utmb.edu. Dr. Bing Tian, Tel: +1 (409) 772-1177; E-mail: bitian@utmb.edu. Dr. Allan R. Brasier, Tel: +1 (608) 263-7371; E-mail: abrasier@wisc.edu.

ABSTRACT

Bromodomain-containing protein 4 (BRD4) represents a promising drug target for anti-inflammatory therapeutics. Herein, we report the design, synthesis, and pharmacological evaluation of novel chromone derivatives *via* scaffold hopping to discover a new class of orally bioavailable BRD4 selective inhibitors. Two potent BRD4 bromodomain 1 (BD1) selective inhibitors **44** (ZL0513) and **45** (ZL0516) have been discovered with high binding affinity (IC$_{50}$ values of 67~84 nM) and good selectivity over other BRD family proteins and distant BD-containing proteins. Both compounds significantly inhibited the expression of Toll-like receptor (TLR3)-induced inflammatory genes *in vitro* and airway inflammation in murine models. The cocrystal structure of **45** in complex with human BRD4 BD1 at a high resolution of 2.0 Å has been solved, offering a solid structural basis for its binding validation and further structure-based optimization. These BRD4 BD1 inhibitors demonstrated impressive *in vivo* efficacy and overall promising pharmacokinetic properties, indicating their therapeutic potential for the treatment of inflammatory diseases.

INTRODUCTION

Epigenetic modifications on DNA, histones and other nuclear proteins regulate gene expression, affect cellular differentiation and contribute to human diseases.[1, 2] Lysine acetylation (KAc) is one of the most broadly studied post translational modifications occurring on histone proteins. This highly dynamic process is regulated by opposing actions of histone acetyl transferases (HATs) and histone deacetylases (HDACs).[3] Histone acetylation also provides binding sites for proteins, especially BD-containing proteins, to promote chromatin reorganization and transcription. There are 61 structurally homologous BDs present in 46 different proteins in the human proteome. BRD4 belongs to BD and extra-terminal (BET) family consisting of four members (BRD2, BRD3, BRD4 and BRDT). Similar to other subfamily of BD-containing proteins, BET members function in epigenetic regulation of gene expression through binding to KAc recognition pocket on histone tails and non-histone proteins.[4-6] BET family proteins, especially BRD4, have emerged as a promising epigenetic target for human diseases and conditions, including cancers,[7] inflammations,[8-14] HIV infection,[15-17] heart failure,[18] and CNS disorders.[19]

A number of BET inhibitors with different chemotypes (e.g. azepines, 3,5-dimethylisoxazoles, pyridones, diazobenzene) have been discovered and developed as depicted in **Figure 1**.[4, 20] Azepine (+)-JQ1 (**1**, **Figure 1**) has been the most widely used tool BRD4 inhibitor, and its analogue I-BET762 (**2**) has been advanced into phase II human clinical trials for neoplasms.[21, 22] RVX-208 (**3**),[23] a BET inhibitor selective for the second BD, has been enrolled into phase III clinical trials for high-risk cardiovascular disease patients with type 2 diabetes mellitus and low levels of high-density lipoprotein. Despite the fact that compound **3** demonstrated tolerability and safety, it failed to meet the primary endpoint – reduction in major

adverse cardiovascular events (MACE).[24] Both ABBV075 (**4**) and BMS986158 (**5**) are developed as pan-BET inhibitors in clinical trials for cancer therapy.[25, 26] It has been reported that BD2 inhibition (e.g., **3**) only modestly affects BET-dependent gene transcription and BD1 selective inhibitors are urgently needed for elucidating bromodomain-specific functions. To date, the availability of BD1 selective inhibitors is very limited, let alone BRD4 BD1 specific ones.[23] To improve the selectivity and extend the application of BRD4 inhibitors, we recently designed and synthesized a series of diphenyldiazene BRD4 inhibitors (e.g., ZL0454, **6** in **Figure 1**) that suppress the TLR3-induced expression of proinflammatory genes (IL-6, ISG54 and Groβ) in human small airway cells *in vitro*, as well as TLR3-induced airway inflammation and neutrophilia in mouse models *in vivo*.[8, 9, 12, 13] Although compound **6** displayed good BRD4 inhibition (IC$_{50}$ values of 49 nM and 35 nM against BRD4 BD1 and BRD4 BD2, respectively) and selectivity over other family members, its pharmacokinetic (PK) profile is not satisfactory with poor orally bioavailability (*F* = 0.46%) and metabolic stability as well as poor aqueous solubility (12.8 µg/mL at pH = 7).[8] To further improve the physicochemical properties of BRD4 inhibitors based on our first-generation lead compound **6**, two approaches were utilized by either replacing the N=N linker with moieties that have more favorable metabolic stability or tuning its core structure to alternative privileged scaffolds with better oral bioavailability. Given our proof-of-concept study of BRD4 in airway inflammation (**3** as a positive control displaying moderate *in vivo* efficacy) and the clinically validated safety profile of compound **3**, we believe through dedicated drug design and structural optimization, new analogues with unique scaffolds based on compound **3** could be achieved to significantly improve their oral bioavailability and the *in vivo* efficacy for the treatment of inflammatory diseases. Herein, we report our application of scaffold hopping to discover a new class of potent, selective and orally available BRD4 inhibitors. The

binding modes of them with BRD4 BD1 have been validated by the cocrystal structural analysis

of the inhibitor in complex with human BRD4 BD1 protein.
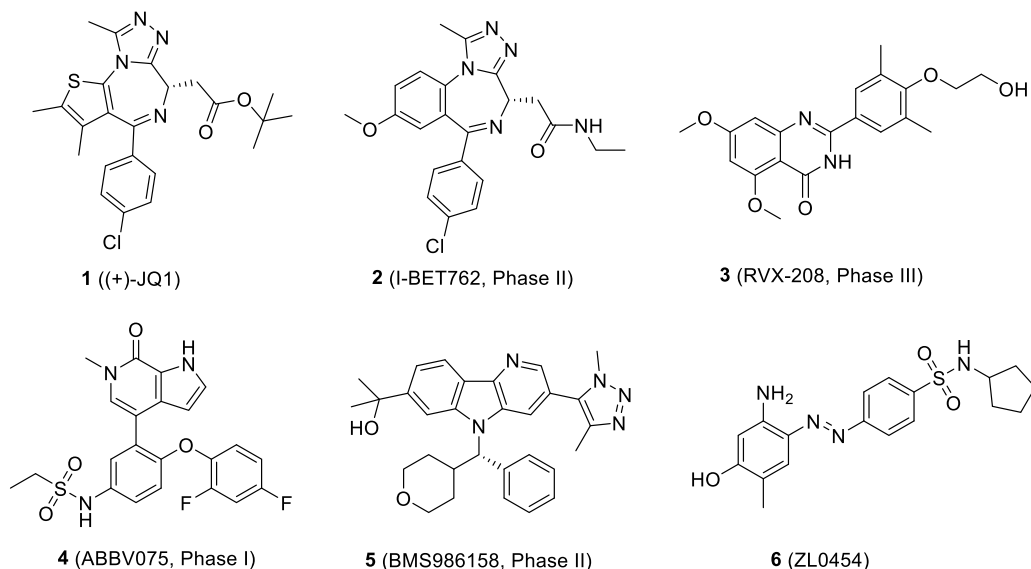
Figure 1. Chemical structures of representative BET inhibitors **1~5** and recently identified BRD4 selective inhibitor **6**.

RESULTS AND DISCUSSION

Design. As depicted in **Figure 2**, the co-crystal structure of compound **3** in complex with

BRD4 BD1 (PDB code: 4MR4) exhibited the lactam of the quinazolin-4-one core, especially the

carbonyl oxygen atom, formed critical H-bonds with Asn140 and Tyr97. The 3,5-dimethylphenol

moiety of compound **3** does not reach the tryptophan-proline-phenylalanine (WPF) shelf but

extends to the upper area of four helix bundle. Interestingly, its analogue RVX-OH (**7**, **Figure 2**)

lacking a 2-hydroxyethyl group was found to interact with BRD4 BD1 in a completely reversed

conformation.[23] The quinazolin-4-one core extends to the WPF shelf area while the oxygen atom

of phenyl group inserted to the critical site forms direct H-bonds with Asn140 and an indirect

interaction with Tyr97, exactly like compound **6**. Such substantial difference may explain why

compound **3** is BD2 selective while compound **7** has no preference between BD1 and BD2.

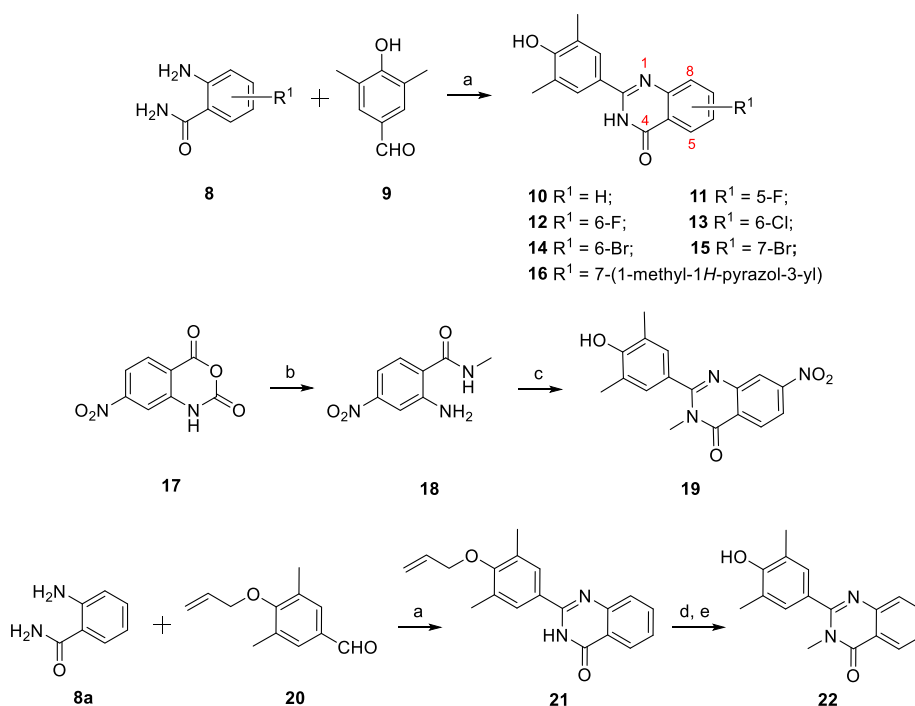Given that its close analogue compound **3**, is clinically proven both safe and metabolically stable, we proposed to optimize substituents on the quinazolin-4-one core of compound **7** (Series I) and the 3,5-dimethylphenol moiety of compound **3** (Series II) to explore whether we can improve the BRD4 BD1 selectivity and achieve a paradigm shift in its clinical application from cardiovascular disease to various inflammatory diseases such as chronic obstructive pulmonary disease (COPD). To accomplish this objective, we used a scaffold hopping strategy to replace the quinazolin-4-one core with chromen-4-one scaffold through fine tuning (Series III) to discover structurally novel BRD4 inhibitors with enhanced potency and BD selectivity as well as an improved drug metabolism pharmacokinetic (DMPK) profile. For series I compounds, they are expected to form the critical interactions with Asn140 and Tyr97 through free -OH like compound **7**, and substitutions on the quinazolin-4-one core can reach the WPF shelf. The relevant structure-activity relationship (SAR) will be helpful to explore the compatibility and possibility to improve potency as well as selectivity at this site. For series II and III compounds, we emphasize the investigations on the side chain which is oriented to a short sequence from Lys91 to Asp 96 in ZA loop which is believed critical for bromodomain selectivity.[27] The short sequence for BRD4 BD1 is KLNLPD (91~96), while it is ALGLHD for BRD4 BD2, KLGLPD for BRD2 BD1, and ALGLHD for BRD2 BD2, respectively. They are not highly conserved, especially Asn93 which is unique for BRD4 BD1. We envision that incorporating proper side chains on the single phenyl ring of series II and III that can critically interact with KLNLPD of BRD4 BD1 domain may achieve a better BD1 selectivity of BRD4.
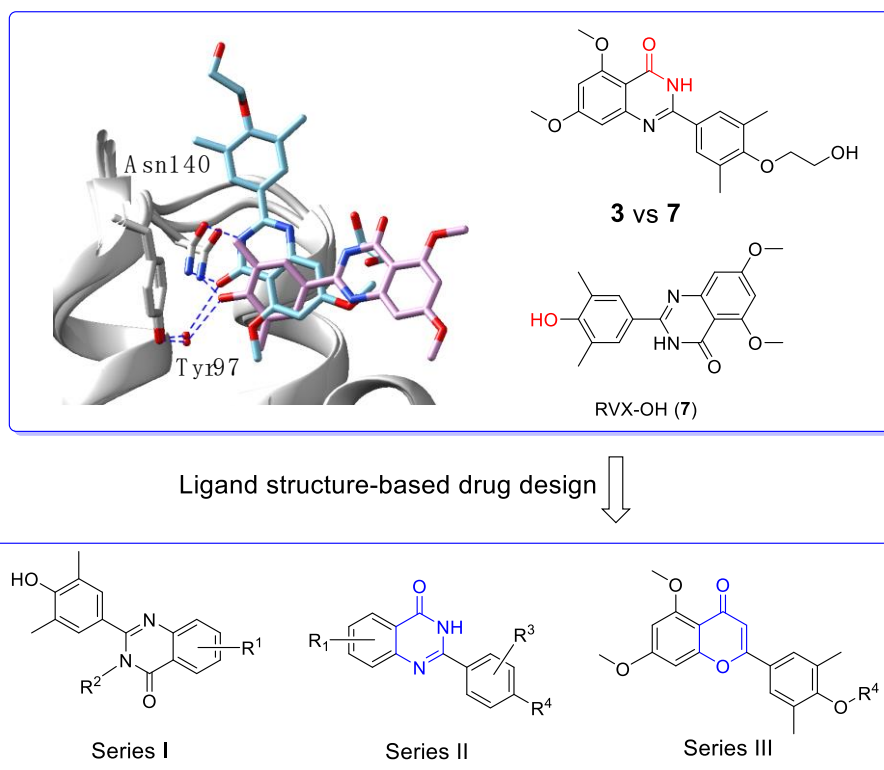
Figure 2. Design of three series of BRD4 inhibitors *via* a ligand structure-based drug design and scaffold hopping strategy. First panel: overlay of cocrystal structures of compounds **3** (in light blue, PDB code: 4MR4) and **7** (in pink, PDB code: 4MR3) with BRD4 BD1. Residues Asn140 and Tyr97 are labeled. Second panel: designed three series of novel compounds to explore the structure-activity relationship (SAR).

Chemistry. The first series of compounds **10~16** were obtained from the reaction of 4-hydroxy-3,5-dimethylbenzaldehyde **9** with various 2-aminobenzamides **8** *via* an efficient, metal-free and I_2-mediated C-N bond formation method (**Scheme 1**).[28] To explore the space tolerance around amide moiety of **7**, a methyl group was introduced through two strategies. 4-Nitro-isotoic anhydride **17** was substituted by CH_3NH_2 to afford intermediate **18** which was readily transformed into desired compound **19** with a methyl group on the amide. After construction of the quinazolin-4-one core *via* allylic-protected benzaldehyde **20**, compound **21** was methylated by CH_3I and deprotected in the presence of $Pd(PPh_3)_4$ and K_2CO_3 smoothly to give compounds **22**.

Scheme 1. **Synthetic Procedure of Series I.**[a]

10 R^1 = H;   11 R^1 = 5-F;
12 R^1 = 6-F;   13 R^1 = 6-Cl;
14 R^1 = 6-Br; 15 R^1 = 7-Br;
16 R^1 = 7-(1-methyl-1H-pyrazol-3-yl)

[a]Reagents and conditions: a) I$_2$, EtOH, reflux, 4 h, 89%~quant. b) CH$_3$NH$_2$, THF, DIPEA; c) 2-aminobenzamide, I$_2$, EtOH, 57% for two steps; d) CH$_3$I, NaH, DMF, rt., overnight, 94%; e) Pd(PPh$_3$)$_4$, K$_2$CO$_3$, CH$_3$OH, reflux, 4 h, 72%.

The synthesis of the second series of compounds is depicted in **Scheme 2**. Compound **24** and **25** were obtained following a similar procedure to that of compounds **10~16** from commercially available starting material 2-aminobenzamide **8a** and various benzaldehydes **23**. Compounds **27~31** were obtained through the reaction of 2-amino-4,6-dimethoxybenzamide **8b** and substituted benzaldehydes **26** (commercially available or slight modification on 4-hydroxy-3,5-dimethylbenzaldehyde **9**). Addition of 1-methylpiperazine with **31** produced **32** in a yield of 35%. Compound **3** was also resynthesized as the reference compound taking the same strategy in a yield of 82% for two steps (**Scheme 3**), while the original synthetic method of compound **3** was reported to take 8 steps with an overall yield of 5% and included harsh conditions like high temperature (170 ˚C) and two gases in pure form (HCl and NH$_3$).[23]

Scheme 2. Synthetic Procedure of Series II.[a]

8a   **23**   **24** R^3 = 2,5-di F   **25** R^3 = 3,5-di OMe

8b   **26**   **27** R^3 = H, R^4 = CF_3;
28 R^3 = 3-Me, R^4 = CF_3;
29 R^3 = H, R^4 = OH;
30 R^3 = 2-Cl, R^4 = OH;
31 R^3 = 3,5-di Me, R^4 =
32 R^3 = 3,5-di Me, R^4 =
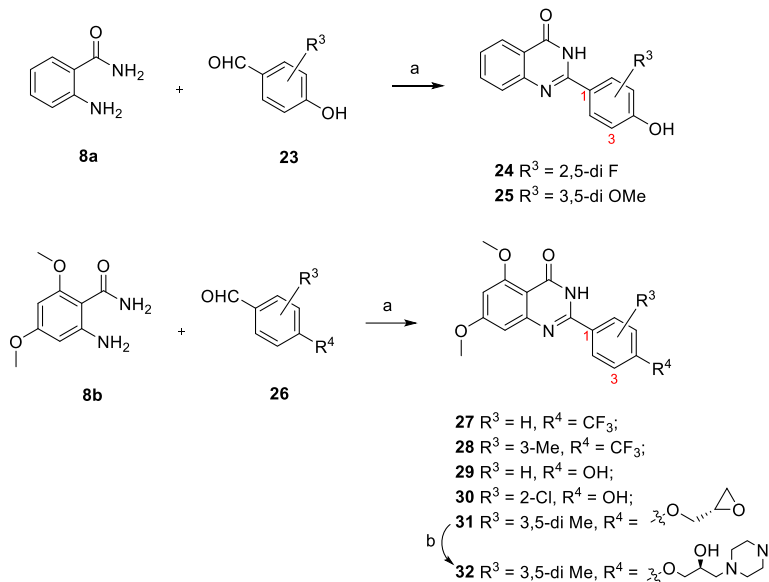
[a]Reagents and conditions: a) I_2, EtOH, reflux, 4 h, 86%~quant. b) 1-methylpiperazine, K_2CO_3, DMF, 90 ˚C, overnight, 35%.

Scheme 3. Resynthesis of Compound 3.[a]

9   **34**   **3**

ref. 22

Our work: 82% (two steps, overall yield)

Previous work: ~ 5% (8 steps, overall yield)
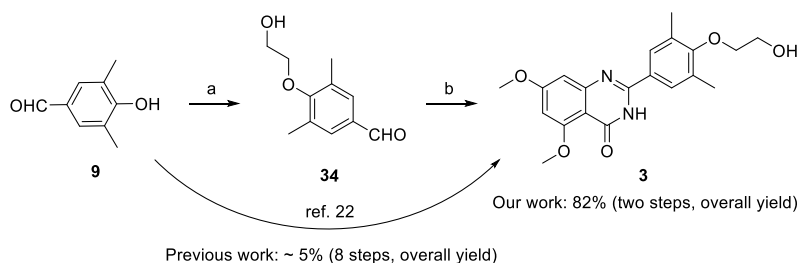
[a]Reagents and conditions: a) 2-bromoethan-1-ol (**33**), K_2CO_3, CH_3CN, reflux, overnight. b) **8b**, I_2, EtOH, reflux, 2 h, 82% (two steps).

The synthetic procedure of series III containing a new chromone core is depicted in **Scheme 4**. Aldol reaction of reagents **20** and **35** gave intermediate **36** which was cyclized under I_2 in DMSO leading to compound **37**. Compound **37** was deprotected in presence of $Pd(PPh_3)_4$ and K_2CO_3 affording critical intermediate **38**. Compound **38** was substituted by 2-bromoethan-1-ol (**33**) to produce compound **39** which is exactly the same with compound **3** except the core. More derivatives **42~49** were obtained via a substitution reaction and cyclic addition. Compound **50**

was obtained through transformation of –OH (**44**) into –F under diethylaminosulfur trifluoride

(DAST) in a yield of 80%.

Scheme 4. Synthetic Procedure of Series III.[a]
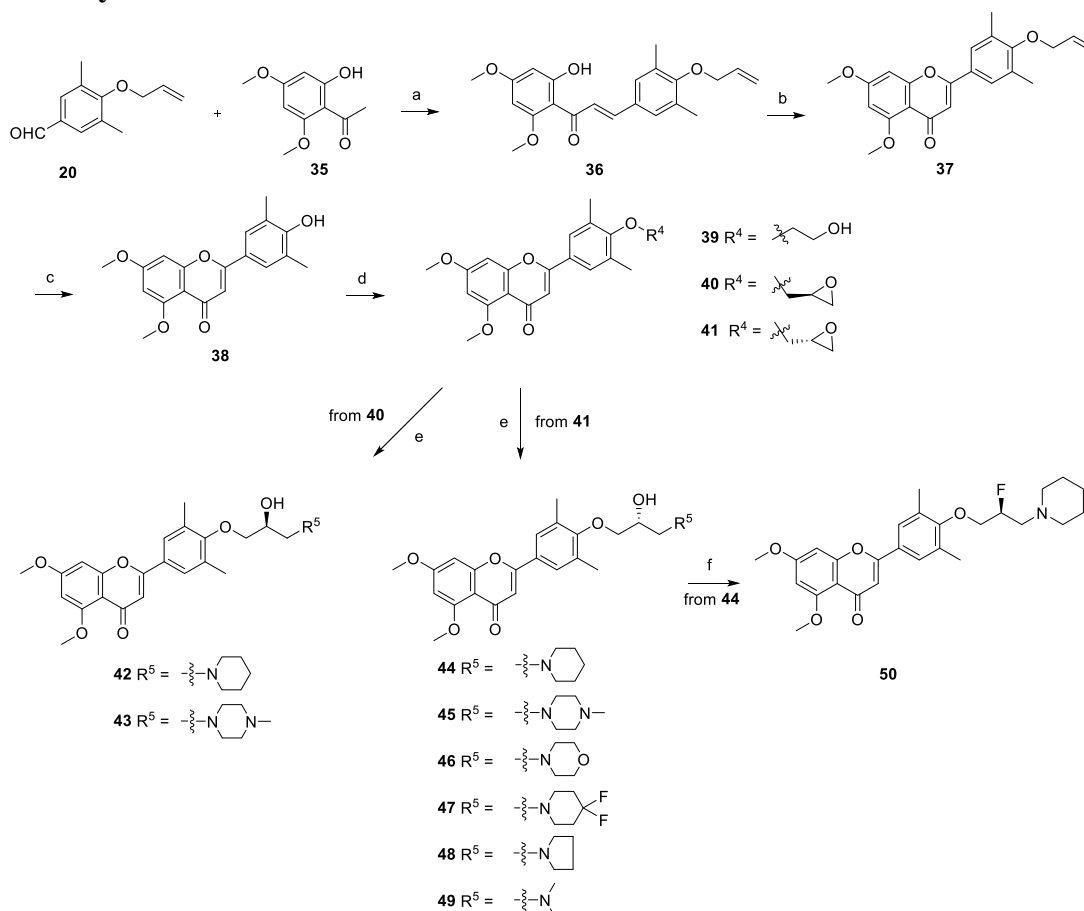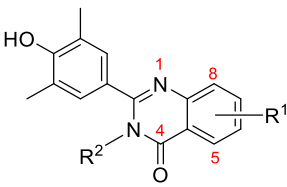
[a]Reagents and conditions: a) 50% KOH, EtOH, rt., overnight, used directly for next step. b) I$_2$, DMSO, 140 °C, 4 h, 36%. c) Pd(PPh$_3$)$_4$, K$_2$CO$_3$, CH$_3$OH, 90 °C, 7 h, 75%. d) R^4-Br, K$_2$CO$_3$, DMF, 80 °C, overnight, 55~72%. e) R^5-H, K$_2$CO$_3$, DMF, 80 °C, overnight, 18%~65% for two steps. f) DAST, CH$_2$Cl$_2$, rt, overnight, 80%.

Inhibitory Activities against TLR3-Induced Expression of Inflammatory Genes *In*

***Vitro*.** All the newly synthesized compounds were first evaluated for inhibitory activity of TLR3

signaling in human small airway epithelial cells (hSAECs) at the concentration of 10 μM, an

assay to demonstrate cellular permeability and BRD4 inhibitory efficacy for further studies.

TLR3-inducible expression of CIG5 and IL-6 genes was determined by quantitative real-time

PCR (qRT-PCR). Percentages of inhibition (%) were calculated based on the level of mRNA expression in poly(I:C)-stimulated cells without compounds.[8] For the first series of compounds, **7** was tested as the positive control. Different halogens at diverse positions and bulky substituents (e.g., 1-methyl-1*H*-pyrazol-3-yl and NO_2) on the quinazolin-4-one core as well as a methyl group on the amide were explored. Despite the finding that compound **7** displayed impressive inhibitory activities of *CIG5* and *IL-6* mRNA induction with inhibition rates of 86% and 75%, respectively, none of its newly synthesized analogues showed obvious improvement (**Table 1**). This suggests that the electron-donating methoxy groups on the phenyl ring are critical for the cellular effects.

Table 1. Inhibitory Rates of Series I Compounds on TLR3-induced Expression of Inflammatory Genes in hSAECs at the concentration of 10 μMª
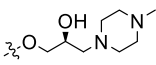
Compounds	R^1	R^2	CIG5 (%)	IL-6 (%)
7	5-OMe 7-OMe	H	86 ± 11	75 ± 8.6
10	H	H	-26 ± 3.1	81 ± 8.9
11	5-F	H	33 ± 4.8	62 ± 7.2
12	6-F	H	-4.5 ± 0.57	62 ± 7.1
13	6-Cl	H	37 ± 4.9	53 ± 5.6
14	6-Br	H	43 ± 6.1	25 ± 3.4
15	7-Br	H	51 ± 6.3	15 ± 1.9
16	7-(1-methyl-1H-pyrazol-3-yl)	H	71 ± 8.5	-24 ± 2.8
19	7-NO_2	CH_3	-69 ± 7.4	86 ± 9.1
22	H	CH_3	18 ± 2.3	55 ± 6.5

ªInhibitory rates (%) are reported as mean ± SD of expression with compound divided by that in solvent (×100). Data are derived from three independent measurements (n = 3).

The second series of compounds were tested using compounds **3** and **7** as the positive controls, which had similar cellular activities (**Table 2**). We first validated the necessity of electron-donating methoxy groups on the quinazolin-4-one core. Consistent with the results of first series of small molecules, compounds **24** and **25** without methoxy groups exhibited obviously decreased activity. Substituents on the single phenyl ring were then explored, and –OH group at 4-position (**29**) was more favored than –CF_3 (**27** and **28**). Replacement of 3,5-dimethyl group with H (**29**) or 2-Cl (**30**) displayed slightly declined inhibitory activities against both poly(I:C)-induced CIG5 and IL-6 expression. Further substituents on 4-OH were investigated, and both compounds **31** and **32** showed equal or better inhibition than **3**, indicating that this position is tolerable for structural optimization.

Table 2. Inhibitory Rates of Series II Compounds on TLR3-induced Expression of Pro-Inflammatory Genes at the concentration of 10 μM[a]
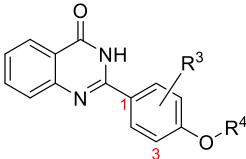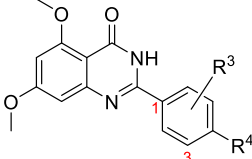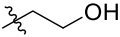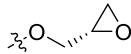

Compounds	R^3	R^4	CIG5 (%)	IL-6 (%)
3	3,5-di Me	⌇⌁OH	84 ± 8.6	65 ± 7.3
7	3,5-di Me	OH	86 ± 9.7	75 ± 8.4
24	2,5-di F	H	2.2 ± 0.37	59 ± 6.8
25	3,5-di OMe	H	61 ± 7.3	59 ± 7.5
27	H	CF_3	45 ± 4.2	-33 ± 4.1
28	CH_3	CF_3	-21 ± 2.9	45 ± 5.7
29	H	OH	81 ± 9.2	63 ± 6.8

30	2-Cl	OH	42 ± 4.8	66 ± 7.5
31	3,5-di Me		87 ± 9.9	83 ± 8.4
32	3,5-di Me		83 ± 8.8	80 ± 9.2

[a]Inhibitory rates (%) are reported as the geometric mean of expression with compound divided by that in solvent (×100). Data are derived from three independent measurements.

The third series of compounds were obtained through a scaffold hopping approach (**Table 3**). Compound **39** exhibited significantly improved inhibition of poly(I:C)-induced CIG5 and IL-6 expression (inhibitory rates of 97% and 98%, respectively) compared to compound **3**, suggesting that the new chromone core appears to be superior to the quinazolin-4-one scaffold. Based on SAR of series II compounds, the side chain on 4-OH was found to be tolerant to modification. Thus, we tried various hydrophilic side chains containing heterocyclic ring capable of increasing the aqueous solubility of the small molecules and constraining its conformation at the same time. Compared to **32**, compounds **43** and **45** with new chromone core displayed a better inhibitory activity (99% against both CIG5 and IL-6). Compounds incorporating piperidine (**42** and **44**) and pyrrole (**48**) exhibited similarly potent effects to 1-methylpiperazine (**43** and **45**), while compounds with moieties of morpholine (**46**), 4,4-difluoropiperidine (**47**) and dimethylamine (**49**) displayed substantially decreased inhibitory activities. *R*- or *S*- configuration of -OH group on the side chain was found to make no significant differences (**42** *vs* **44** and **43** *vs* **45**). Fluorine is widely used to improve the metabolic stability in drug discovery process[29] and the replacement of –OH of **44** with –F (**50**) showed slightly declined inhibition against poly(I:C)-induced CIG5 and IL-6 expression compared to that of compound **44**.

Table 3. Inhibitory Rates of Series III Compounds on TLR3-induced Expression of Pro-Inflammatory Genes at the concentration of 10 μM[a]

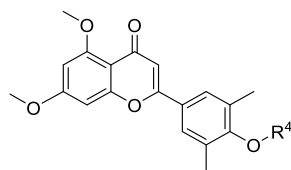| Compounds	R^4	CIG5 (%)	IL-6 (%)
3	$\sim$OH	84 ± 8.8	65 ± 5.7
37	$\sim$	83 ± 7.7	NT^b
39	$\sim$OH	97±10.5	98±11.4
42	OH, piperidine	100 ± 9.8	100 ± 11
43	OH, N-methylpiperazine	99 ± 11	99 ± 9.2
44	OH, piperidine	99 ± 12	100 ± 11
45	OH, N-methylpiperazine	91 ± 10	97 ± 9.3
46	OH, morpholine	42 ± 5.1	82 ± 9.6
47	OH, 4,4-difluoropiperidine	63 ± 7.5	88 ± 9.3
48	OH, pyrrolidine	92 ± 11	99 ± 11
49	OH, dimethylamine	-19 ± 2.5	82 ± 7.7
50	F, piperidine	85 ± 9.3	90 ± 8.6

^{a}Inhibitory rates (%) are reported as the geometric mean of expression with compound divided by that in solvent (×100). Data are derived from three independent measurements. ^{b}NT: Not tested.

IC$_{50}$ values were calculated for selected active compounds **39**, **42**-**45** and **48** displaying potent inhibition against both genes with inhibitory rates over 90% (**Table 4**). Compound **32** with quinazolin-4-one core was also included for comparison. Positive control **1** exhibited IC$_{50}$ values of 0.92 μM and 1.02 μM against poly(I:C)-induced CIG5 and IL-6 expression,

respectively. Compounds **32** and **39** displayed 2 to 4-fold decreased IC_{50} values which were comparable to compound **3**. Compounds **42~45** exhibited significantly improved effects with submicromolar cellular IC_{50} values, while compound **48** displayed IC_{50} values around 1 μM comparable to that of reference compounds **1** and **3**. The most potent compound **45** showed excellent IC_{50} values of 280 nM and 310 nM against poly(I:C)-induced CIG5 and IL-6 expression, respectively (**Table 4**).

Table 4. IC_{50} Values of Selected Compounds against TLR3-Induced Expression of Inflammatory Genes[a]

Compd	CIG5 (μM)	IL-6 (μM)
1	0.95 ± 0.11	1.02 ± 0.10
3	1.66 ± 0.15	3.29 ± 0.41
32	2.6 ± 0.22	3.5 ± 0.33
39	2.6 ± 0.21	2.8 ± 0.32
42	0.58 ± 0.49	0.54 ± 0.47
43	0.83 ± 0.07	0.75 ± 0.08
44	0.52 ± 0.05	1.1 ± 0.12
45	0.28 ± 0.03	0.31 ± 0.02
48	1.48 ± 0.17	0.97 ± 0.09

[a]IC_{50} values are reported as the mean concentration (μM) derived from three independent measurements. Each titration curve was generated from at least 8 different concentrations.

Binding Affinities of Selected Compounds towards BET BDs. Compounds **42**, **43**, **44** and **45** were selected for further studies to determine binding affinities with BET BDs and non-BET proteins *via* time-resolved fluorescence energy transfer (TR-FRET) assay. Results of positive controls **1** and **3** were consistent with reported data which reflected the reliability of our assay. Compounds **42**-**45** showed about a 10-fold increase in potency over compound **3** for BRD4 BD1 binding. Compounds **42** and **43** are BRD4 selective without preference for BRD4 BD1 and BRD4 BD2, while both compounds **44** and **45** exhibited a good selectivity for BRD4 BD1 over other BET BDs, including BRD4 BD2. Besides, compound **45** displayed good selectivity over non-BET bromodomain-containing proteins (**Table S1**). Meanwhile, no obvious off-target

effects of **45** were observed from the NIMH psychoactive drug screening program (PDSP) using

a wide panel of target screening (**Table S2**).

**Table 5. Binding Affinities of Selected Compounds for the BET BDs and Non-BET Protein CBP (nM)**[a]

BDs	1	3	42	43	44	45
BRD4 BD1	92 ± 7.8	1,142 ± 98	86 ± 7.8	127 ± 14	67 ± 5.4	84 ± 7.3
BRD4 BD2	62 ± 5.9	135 ± 14	93 ± 8.5	139 ± 12	684 ± 7.5	718 ± 69
BRD2 BD1	78 ± 7.2	5,780 ± 463	1,205 ± 116	1,286±113	791±67	886±75
BRD2 BD2	52 ± 5.5	251 ± 186	1,196 ± 97	1,437 ± 156	845 ± 73	914 ± 81
BRD3 BD1	81 ± 7.4	3,962 ± 317	1,906 ± 173	2,631 ± 197	2,395 ± 198	3,122 ± 285
BRD3 BD2	69 ± 5.7	203 ± 19	1,719 ± 156	1,962 ± 159	2,081 ± 186	2,495 ± 217
BRDT BD1	183 ± 16	4,836 ± 457	2,502 ± 195	2,765 ± 237	2,869 ± 257	3,592 ± 293
BRDT BD2	217 ± 23	708 ± 69	2,411 ± 207	2,545 ± 236	2,317 ± 206	3,176 ± 276
CBP	9,600 ± 785	>10,000	>10,000	>10,000	>10,000	>10,000

[a]Binding affinity was measured using a TR-FRET assay with the isolated recombinant BD. Reported as mean ± SD from three separate assay runs (n = 3).

Co-crystal Structure Analysis of Compound 45 in Complex with Human BRD4 BD1.

To gain more insight into the binding modes of compound **45** with BRD4 BD1 and validate the

efficiency of the scaffold hopping strategy, we have successfully solved a high resolution co-

crystal structure of **45** in complex with BRD4 BD1 at 2 Å (PDB code: 6UWU; **Figure 3, S1** and

Table S3). Similar to the binding mode shown by compound **3**, the new inhibitor **45** occupied

the classical KAc recognition site very well with the aid of several water molecules (**Figure 3A**).

The carbonyl O atom interacted with Asn140 directly and formed an indirect hydrogen bond

with Tyr97 mediated by a water molecule. One methoxy group on the chromone core was

accommodated in the pocket by a hydrogen bond mediated with water, while the other methoxy

group extended to the WPF shelf area which was consistent with SAR analysis indicating the

critical role of –OMe moieties. The 1-methylpiperazine was excluded from the pocket and

reached the solvent area consistent with the SAR and perfectly explaining why side chain

modifications were tolerated (**Figure 3B**). The chiral –OH on the side chain is in proximity of a

water molecule where it forms a water-mediated hydrogen bond with Asn93 (**Figure 3C**). The

equivalent residue of Asn93 on BRD4 BD2 is a glycine, and thus this hydrogen bond interaction

is missing for BRD4 BD2 with **45**. Similarly, the equivalent residues of Asn93 are glycine for

BRD2 BD1, glycine for BRD2 BD2, glutamic acid for BRD3 BD2, glutamine for BRDT BD1

and glycine for BRDT BD2, respectively. This may explain the selectivity of **45** over

bromodomains of BET family members. Although BRD3 BD1 has the same asparagine, the

overall ZA loop shift (as far as 5~8 Å) is obvious thereby allowing the KAc recognition pocket

much larger than BRD4 BD1 (Figure S2). Therefore, it is likely more difficult for the compound

adhering to the residues. This speculation is consistent with the previous reported results from

Morelli group.[27] Overlay analysis of the crystal structures of **3** and **45** with BRD4 BD1

demonstrated a highly conserved pose except for the flexible side chain on 4-OH (**Figure 3D**).

These findings validated and supported the high reliability and feasibility of our scaffold hopping

strategy.
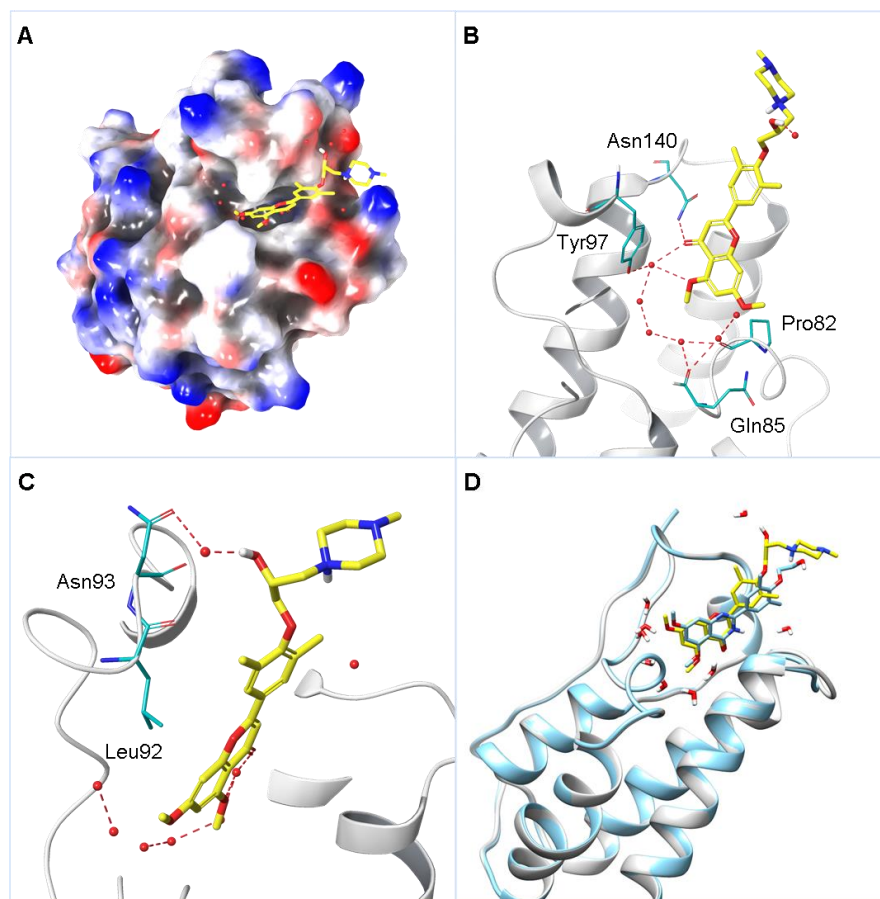
Figure 3. (**A**) Crystal structure of **45** (in yellow) in co-complex with human BRD4 BD1 (PDB code: 6UWU) in representation of electrostatic potential surface. (**B**) Critical interactions of **45** with BRD4 BD1. Residues Asn140, Tyr97 and Pro82 are highlighted in light blue and hydrogen bonds are colored in red. (**C**) Zoomed details around chiral –OH. Residues Asn93 and Leu92 are highlighted in light blue. (**D**) Overlay analysis of **3** (in light blue, PDB code: 4MR4) and **45** (in yellow) in co-complex with human BRD4 BD1 in ribbon representation.

Drug-like Properties of BRD4 BD1 Inhibitors 44 and 45. With promising *in vitro* activities in hand, we then studied the *in vivo* PK profiles of compounds **44** and **45**. As listed in **Table 6** and depicted in **Figure S3**, these inhibitors displayed similar but overall favorable PK parameters (3 to 4 hours of half-life, maximum concentration around 600 ng/mL and AUC values of about 5,000 ng·h/mL). The ultimate oral bioavailability of compounds **44** and **45** are 38% and 35%, respectively, indicating both compounds are orally available. Moreover, both compounds have an excellent aqueous solubility with concentrations > 50 mg/mL. Furthermore,

compound **45** is metabolically stable in the liver microsomes stability assay and CYP450

inhibition study. The clearance rates were 25 and 5.6 µL/min/mg for mouse liver microsomes

(MLM) and human liver microsomes (HLM), respectively. The unbound fractions of compound

45 are 12% and 17% in mouse and human plasma protein binding, respectively, which is

reasonable to drive the pharmacological effects. In addition, no obvious inhibitor effects were

found on either hERG or CYP450 enzymes including CYP 3A4, 1A2, 2C9, 2D6, 2C19, 2C8 or

2B6 at the concentration of 10 µM (**Table 7**). Taken together, these BRD4 BD1 inhibitors

demonstrated impressive overall drug-like properties to support their further clinical

development.

Table 6. *In Vivo* PK Profiles of Compounds 44 and 45 in Rats.[a]

		44	**45**
i.v. (10 mg/kg)	[b]$t_{1/2}$ (h)	3.5 ± 0.71	4.1 ± 0.43
	[c]C_{max} (ng/mL)	$2,861 \pm 426$	$2,090 \pm 265$
	[d]AUC_{0-t} (ng·h/mL)	$6,763 \pm 590$	$7,033 \pm 2161$
	[e]CL (L/hr/kg)	1.48 ± 0.13	1.48 ± 0.38
p.o. (20 mg/kg)	$t_{1/2}$ (h)	2.4 ± 0.55	2.8 ± 0.27
	C_{max} (ng/mL)	575.1 ± 179	605.5 ± 182
	AUC_{0-t} (ng·h/mL)	$5,171 \pm 3447$	$4,966 \pm 1772$
	[f]F (%)	38.2	35.3

[a]Compounds were formulated in 10%DMSO/60%PEG400/30%Saline and administrated intravenously (i.v.) or per os (p.o.). [b]$t_{1/2}$, half-life. [c]C_{max}, maximum plasma concentration achieved. [d]AUC_{0-t}, total exposure following single dose. [e]CL, total clearance. [f]F, oral bioavailability.

Table 7. *In Vitro* Liver Microsomes Stability Assay, Cytochrome P450 Enzymes and hERG

Inhibition Assay[a]

Compound	**45**
MLM (CL, µL/min/mg)	25
HLM (CL, µL/min/mg)	5.6
Mouse plasma protein binding (free fraction, %)[b]	12
Human plasma protein binding (free fraction, %)	17
CYP 3A4(MDZ)[c]	9.5 ± 5.6
CYP 3A4(Testo)[d]	8.2 ± 2.1
CYP 1A2	0.0 ± 0.0

CYP 2C9	1.9 ± 0.25
CYP 2D6	0.0 ± 0.0
CYP 2C19	1.7 ± 0.29
CYP 2C8	17 ± 3.0
CYP 2B6	27 ± 4.3
hERG (IC_{50}, μM)	> 30

[a]Inhibitory rates (%) on CYP450 enzyme at the concentration of 10 μM. [b]Concentration is 2 μM [c]Substrate is midazolam (MDZ). [d]Substrate is testosterone (Testo).

In Vivo **Efficacy of Selected BRD4 BD1 Inhibitors 44 and 45.** Next, compounds **44** and

45 were investigated in our established murine model of TLR3-induced acute airway

inflammation.[8, 12] Both oral administration (p.o.) and intraperitoneal administration (i.p.) were

employed to compare their *in vivo* efficacy. Vehicle alone and poly (I:C)-treated groups were

tested as healthy and pathological controls, respectively. Histologically, we observed that

poly(I:C) induced a profound neutrophilic inflammation around the small- and medium-sized

airways which was completely inhibited by two inhibitors at the dose of 10 mg/kg *via* p.o. or i.p.

administration respectively (**Figure 4A**). Meanwhile, elevated secretion of total cells and

neutrophils (**Figure 4B**) was suppressed, and inflammatory cytokines (IL-6, KC, MCP-1, and

RANTES, **Figure 4C**) in bronchoalveolar lavage fluid (BALF) were also significantly blocked.

We also measured inflammatory gene expression in lung tissue (**Figure 4D**). Administration of

poly(I:C)-induced 15- to 20-fold increase of inflammatory genes IL-6, KC, ISG54 and CIG5 in

lung tissue. Compounds **44** and **45** were found to inhibit these increases significantly. These

results validated the potent *in vivo* efficacy of our newly designed compounds achieved from the

scaffold hopping approach. To further validate their *in vivo* efficacy actually induced by

inhibiting BRD4 rather than any other off-target effects, we examined the level of H3K122Ac

which is verified as a BRD4 biomarker (**Figure 5**).[10,12,13] Immunofluorescence staining of

H3K122Ac demonstrated that poly(I:C) induced significant increase of BRD4 activities in both

hSAECs and lung tissue of mice, and this poly(I:C)-induced effect was effectively blocked by

BRD4 inhibitors **44** and **45** through the down-regulation of H3K122Ac.
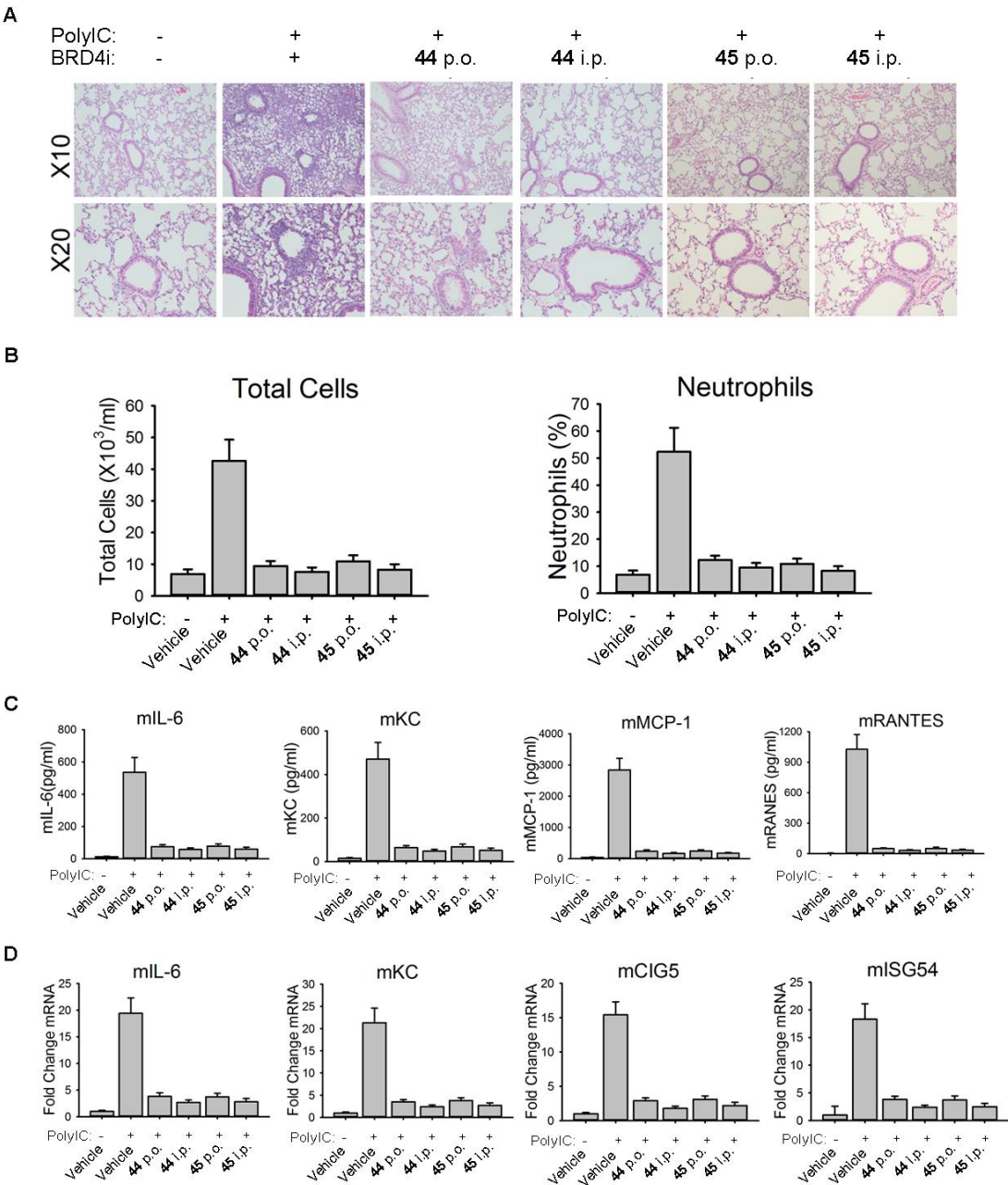
Figure 4. *In vivo* **efficacy of BRD4 BD1 inhibitors 44 and 45 in poly(I:C)-induced airway inflammation of mice.** (**A**) C57BL6/J mice were pre-treated (i.p. or p.o.) with **44** and **45** at the dose of 10 mg/kg before intranasal (i.n.) poly(I:C) exposure. Lung histology images of Hematoxylin and Eosin (H&E) staining were performed on paraffin-embedded lung sections and were shown at magnitude of × 10 and × 20 respectively. (**B**) BRD4 inhibitors **44** and **45** blocked poly(I:C)-induced secretion of inflammatory cells in BALF. (**C**) BRD4 inhibitors blocked

poly(I:C)-induced secretion of inflammatory cytokines in BALF. (**D**) BRD4 inhibitors blocked poly(I:C)-induced inflammatory gene expression in lung tissue.
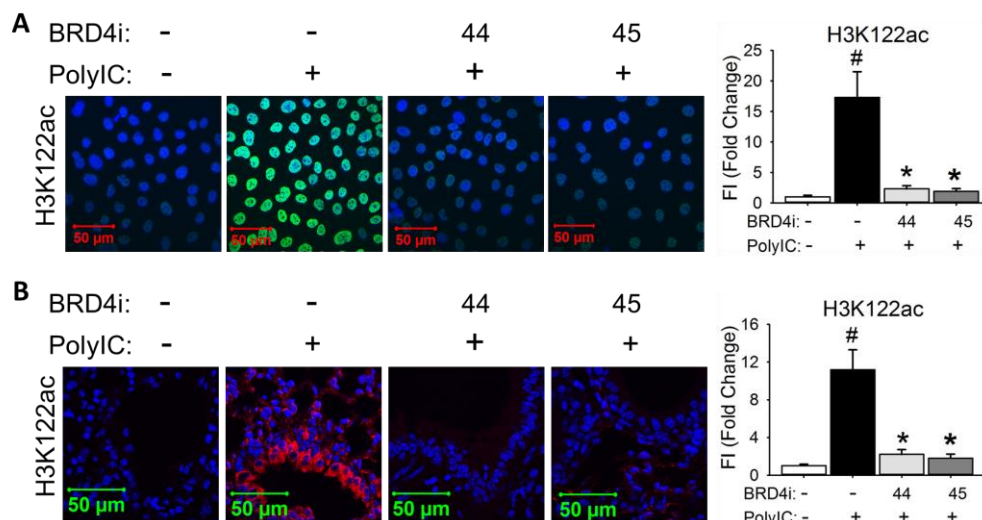
Figure 5. BRD4 inhibitors **44** and **45** block poly(I:C)-induced H3K122Ac in hSAECs (**A**) and in lung tissue of mice (**B**). A) Immunofluorescence staining of H3K122Ac (green) were performed in hSAECs. B) Immunofluorescence staining of H3K122Ac (red) were performed on paraffin-embedded lung sections of mice. Right panel, quantification of total fluorescence intensity shown as fold changes on immunofluorescence staining of H3K122Ac. #$p < 0.01$, compared with control; *$p < 0.01$ compared with poly(I:C) only, n = 5.

CONCLUSION

In summary, we have discovered a series of novel chromone derivatives as potent and selective BRD4 BD1 inhibitors *via* a scaffolding hopping strategy. Among them, compounds **44** (ZL0513) and **45** (ZL0516) displayed potent cellular effects with submicromolar IC$_{50}$ values, nanomolar binding affinity of 67~84 nM with BR4 BD1 and good selectivity as well as significant *in vivo* efficacy in blocking poly(I:C)-induced airway inflammation and neutrophilia of mice. Co-crystal structure of **45** in complex with human BRD4 BD1 validated its classical KAc recognition site with critical hydrogen bonds to Asn140 and Tyr97. At the same time, both BRD4 BD1 inhibitors **44** and **45** demonstrated excellent DMPK properties including bioavailability >35%, aqueous solubility, metabolic stability, and weak to low CYP450 enzymes and hERG inhibitory effects.

Collectively, the findings support these BRD4 BD1 inhibitors with impressive overall profiles of *in vivo* efficacy and drug-like properties as promising advanced lead compounds for the further optimization and extensive clinical development towards epigenetic therapeutics for the treatment of inflammatory diseases.

EXPERIMENTAL SECTION

General Chemistry Information. All commercially available starting materials and solvents were reagent grade, and used without further purification unless otherwise specified. Reactions were performed under a nitrogen atmosphere in dry glassware with magnetic stirring. Preparative column chromatography was performed using silica gel 60, particle size 0.063-0.200 mm (70-230 mesh, flash). Analytical TLC was carried out employing silica gel 60 F254 plates (Merck, Darmstadt). Visualization of the developed chromatograms was performed with detection by UV (254 nm). NMR spectra were recorded on a Bruker-600 or Bruker-300 (^{1}H, 600 & 300 MHz; ^{13}C, 150 & 75 MHz) spectrometer. ^{1}H and ^{13}C NMR spectra were recorded with TMS as an internal reference. Chemical shifts were expressed in ppm, and *J* values were given in Hz. High-resolution mass spectra (HRMS) were obtained from Thermo Fisher LTQ Orbitrap Elite mass spectrometer. Parameters include the following: Nano ESI spray voltage was 1.8 kV; Capillary temperature was 275 °C and the resolution was 60,000; Ionization was achieved by positive mode. Purities of final compounds were established by analytical HPLC, which was carried out on a Shimadzu HPLC system (model: CBM-20A LC-20AD SPD-20A UV/VIS). HPLC analysis conditions: Waters μBondapak C18 (300 × 3.9 mm); flow rate 0.5 mL/min; UV detection at 270 and 254 nm; linear gradient from 10% acetonitrile in water to 100% acetonitrile

in water in 20 min followed by 30 min of the last-named solvent (0.1% TFA was added into both acetonitrile and water). All biologically evaluated compounds are > 95% pure.

2-(4-Hydroxy-3,5-dimethylphenyl)quinazolin-4(3*H*)-one (10). To a solution of 2-aminobenzamide (136 mg, 1.0 mmol) and 4-hydroxy-3,5-dimethylbenzaldehyde (180 mg, 1.2 mmol) in 10 mL EtOH, I_2 (279 mg, 1.1 mmol) was added. After reflux for 4 h, 5% $Na_2S_2O_4$ was added to quench the reaction. Compound **10** (266 mg, quant.) was obtained through filtration as a white solid. HPLC purity 95.7% (t_R = 13.13 min). ^{1}H NMR (300 MHz, DMSO-d_6) δ 12.10 (s, 1H), 8.11 (d, *J* = 7.9 Hz, 1H), 7.86 (s, 2H), 7.79 (t, *J* = 7.6 Hz, 1H), 7.68 (d, *J* = 8.1 Hz, 1H), 7.45 (t, *J* = 7.7 Hz, 1H), 2.25 (s, 6H). ^{13}C NMR (75 MHz, DMSO-d_6) δ 162.7, 157.0, 152.8, 149.4, 134.9, 128.5, 127.4, 126.3, 124.7, 123.4, 121.0, 17.1. HR ESI-MS $(M + H)^+$ m/z = 267.1134 (calcd for $C_{16}H_{15}N_2O_2$: 267.1127).

5-Fluoro-2-(4-hydroxy-3,5-dimethylphenyl)quinazolin-4(3*H*)-one (11). Compound **11** (71 mg, quant.) was obtained as a white solid following the procedure of **10**. HPLC purity 95.4% (t_R = 13.97 min). ^{1}H NMR (300 MHz, DMSO-d_6) δ 12.15 (s, 1H), 9.00 (s, 1H), 7.85 (s, 2H), 7.79 − 7.67 (m, 1H), 7.49 (d, *J* = 8.1 Hz, 1H), 7.17 (dd, *J* = 10.9, 8.2 Hz, 1H), 2.24 (s, 6H). ^{13}C NMR (75 MHz, DMSO-d_6) δ 162.8, 160.0, 159.3, 157.3, 153.7, 151.7, 135.4, 135.3, 128.6, 124.7, 123.7, 122.9, 112.6, 112.4, 110.4, 17.18. HR ESI-MS $(M + H)^+$ m/z = 285.1029 (calcd for $C_{16}H_{14}FN_2O_2$: 285.1039).

6-Fluoro-2-(4-hydroxy-3,5-dimethylphenyl)quinazolin-4(3*H*)-one (12). Compound **12** (74 mg, quant.) was obtained as a white solid following the procedure of compound **10**. HPLC purity 96.1% (t_R = 14.52 min). ^{1}H NMR (300 MHz, DMSO-d6) δ 12.27 (s, 1H), 8.95 (d, J = 2.8 Hz, 1H), 7.83 (s, 2H), 7.76 (dq, J = 9.0, 5.7, 4.1 Hz, 2H), 7.67 (dd, J = 8.5, 2.5 Hz, 1H), 2.24 (s, 6H). ^{13}C NMR (75 MHz, DMSO-d_6) δ 162.1, 161.6, 158.4, 157.0, 152.2, 146.4, 130.4, 130.3,

128.5, 124.7, 123.5, 123.3, 123.2, 122.2, 122.1, 111.0, 110.7, 17.1. HR ESI-MS (M + H)$^+$ m/z = 285.1031 (calcd for C$_{16}$H$_{14}$FN$_2$O$_2$: 285.1039).

6-Chloro-2-(4-hydroxy-3,5-dimethylphenyl)-3-methylquinazolin-4(3*H*)-one **(13).** Compound **13** (322 mg, quant.) was obtained as a yellow solid following the procedure of compound **10**. ^{1}H NMR (300 MHz, DMSO-d_6) δ 12.29 (s, 1H), 8.97 (s, 1H), 8.02 (d, J = 2.6 Hz, 1H), 7.84 (s, 2H), 7.78 (dd, J = 8.7, 2.5 Hz, 1H), 7.68 (d, J = 8.7 Hz, 1H), 2.24 (s, 6H). ^{13}C NMR (75 MHz, DMSO) δ 161.8, 157.2, 153.2, 148.2, 134.9, 130.4, 129.7, 128.6, 125.2, 124.7, 123.2, 122.2, 17.1. HR ESI-MS (M + H)$^+$ m/z = 301.0749 (calcd for C$_{17}$H$_{16}$ClN$_2$O$_2$: 301.0744).

6-Bromo-2-(4-hydroxy-3,5-dimethylphenyl)quinazolin-4(3*H*)-one (14). Compound **14** (384 mg, quant.) was obtained as a white solid following the procedure of compound **10**. HPLC purity 98.4% (t_R = 17.23 min). ^{1}H NMR (300 MHz, DMSO-d_6) δ 12.33 (s, 1H), 8.99 (s, 1H), 8.17 (d, J = 2.4 Hz, 1H), 7.91 (dd, J = 8.7, 2.4 Hz, 1H), 7.85 (s, 2H), 7.63 (d, J = 8.7 Hz, 1H), 2.24 (s, 6H). ^{13}C NMR (75 MHz, DMSO-d_6) δ 161.6, 157.2, 153.3, 148.6, 137.7, 130.0, 128.6, 128.6, 128.3, 124.7, 124.7, 123.2, 123.1, 122.6, 118.5, 17.09, 17.05. HR ESI-MS (M + H)$^+$ m/z = 345.0225 (calcd for C$_{16}$H$_{14}$BrN$_2$O$_2$: 345.0239).

6-Bromo-2-(4-hydroxy-3,5-dimethylphenyl)-3-methylquinazolin-4(3*H*)-one **(15).** Compound **15** (340 mg, 94%) was obtained as a brown solid following the procedure of compound **10**. HPLC purity 96.1 % (t_R = 17.54 min). ^{1}H NMR (300 MHz, DMSO-d_6) δ 8.00 (dd, J = 8.4, 1.9 Hz, 1H), 7.86 (d, J = 4.3 Hz, 3H), 7.59 (d, J = 8.4 Hz, 1H), 2.29 – 2.16 (m, 6H). ^{13}C NMR (75 MHz, DMSO-d_6) δ 162.4, 157.3, 154.2, 150.7, 129.7, 129.1, 128.7, 128.4, 128.3, 124.7, 123.1, 120.1, 17.1. HR ESI-MS (M + H)$^+$ m/z = 345.0236 (calcd for C$_{17}$H$_{16}$BrN$_2$O$_2$: 345.0239).

2-(4-Hydroxy-3,5-dimethylphenyl)-7-(1-methyl-1*H*-pyrazol-5-yl)quinazolin-4(3*H*)-one (16). Compound **16** (70 mg, 89%) was obtained as a brown solid following the procedure of compound **10**. HPLC purity 95.8 % (t_R = 14.74 min). ^{1}H NMR (300 MHz, DMSO-d_6) δ 12.25 (s, 1H), 8.98 (s, 1H), 8.18 (d, *J* = 8.1 Hz, 1H), 7.89 (s, 2H), 7.81 (s, 1H), 7.61 (d, *J* = 8.2 Hz, 1H), 7.53 (d, *J* = 2.1 Hz, 1H), 6.61 (d, *J* = 2.3 Hz, 1H), 3.97 (s, 3H), 2.25 (s, 6H). ^{13}C NMR (75 MHz, DMSO-d_6) δ 162.4, 157.2, 153.5, 149.8, 142.1, 138.6, 136.3, 128.6, 126.9, 126.2, 124.7, 123.3, 120.4, 107.2, 38.4, 17.1. HR ESI-MS (M + Na)$^+$ m/z = 369.1333 (calcd for $C_{20}H_{19}N_4O_2$: 369.1327).

2-(4-Hydroxy-3,5-dimethylphenyl)-3-methyl-7-nitroquinazolin-4(3*H*)-one (19). To a solution of 7-nitro-2*H*-benzo[*d*][1,3]oxazine-2,4(1*H*)-dione (416 mg, 2.0 mmol) in 20 mL THF, DIPEA (516 mg, 4.0 mmol) and CH_3NH_2 (544 mg, 8.0 mmol) were added at room temperature. After 2 h, the solution was poured in to a 0.5 M HCl solution and extracted by CH_2Cl_2. The organic phase was dried over anhydrous Na_2SO_4 and concentrated to get crude 2-amino-*N*-methyl-4-nitrobenzamide **18** which was used directly in the next step. Compound **19** (186 mg, 57% for two steps) was obtained from 2-amino-*N*-methyl-4-nitrobenzamide following the procedure of **10** as a yellow solid. HPLC purity 98.8% (t_R = 16.66 min). ^{1}H NMR (300 MHz, DMSO-d_6) δ 8.84 (s, 1H), 8.31 (d, *J* = 8.6 Hz, 2H), 8.17 (d, *J* = 8.8 Hz, 1H), 7.27 (s, 2H), 3.43 (s, 3H), 2.23 (s, 6H). ^{13}C NMR (75 MHz, DMSO-d_6) δ 161.5, 159.1, 155.7, 151.5, 147.9, 129.1, 128.9, 125.8, 124.6, 124.3, 122.5, 120.3, 35.1, 17.0. HR ESI-MS (M + H)$^+$ m/z = 326.1147 (calcd for $C_{17}H_{16}N_3O_4$:326.1141).

2-(4-(Allyloxy)-3,5-dimethylphenyl)quinazolin-4(3*H*)-one (22). Compound **21** was obtained as a white solid following the procedure of **10**. To a solution of compound **21** (153 mg, 0.5 mmol) and CH_3I (142 mg, 1.0 mmol) in 3 mL of DMF, NaH (24 mg, 1.0 mmol) was added.

After 4 hours, the mixture was poured into iced water and extracted by CH_2Cl_2. The combined organic layer was concentrated and purified by PTLC to give 2-(4-(allyloxy)-3,5-dimethylphenyl)-3-methylquinazolin-4(3H)-one as a white solid. To a solution of 2-(4-(allyloxy)-3,5-dimethylphenyl)-3-methylquinazolin-4(3H)-one (100 mg, 0.31 mmol) in 5 mL of CH_3OH, Pd(PPh$_3$)$_4$ (11 mg, 0.01 mmol) and K_2CO_3 (171 mg, 1.24 mmol) were added. After reflux for 4 h, the mixture was poured in to a 0.5 M HCl solution and extracted by CH_2Cl_2. The organic phase was dried over anhydrous Na_2SO_4 and concentrated to get a crude product which was purified by silica gel column chromatography (CH_2Cl_2/MeOH = 20/1 to 10/1) to provide the desired product (62 mg, 72%) as a grey solid. HPLC purity 98.6 % (t_R = 15.6 min). ^{1}H NMR (300 MHz, DMSO-d_6) δ 8.15 (d, J = 7.9 Hz, 1H), 7.86 – 7.75 (m, 1H), 7.64 (d, J = 8.5 Hz, 1H), 7.52 (d, J = 8.1 Hz, 1H), 7.25 (s, 2H), 3.42 (s, 3H), 2.23 (s, 6H). ^{13}C NMR (75 MHz, DMSO-d_6) δ 162.4, 157.0, 155.7, 155.7, 147.7, 134.6, 129.0, 127.5, 126.8, 126.5, 126.1, 124.6, 120.2, 34.7, 17.1. HR ESI-MS (M + H)$^+$ m/z = 281.1282 (calcd for $C_{17}H_{17}N_2O_2$: 281.1290).

2-(2,5-Difluoro-4-hydroxyphenyl)quinazolin-4(3H)-one (24). Compound **24** (120 mg, 88%) was obtained as a light yellow solid following the procedure of **10**. HPLC purity 95.7% (t_R = 6.74 min). ^{1}H NMR (300 MHz, DMSO-d_6) δ 12.29 (s, 1H), 8.14 (d, J = 8.1 Hz, 1H), 7.83 (t, J = 7.8 Hz, 1H), 7.70 (d, J = 8.2 Hz, 1H), 7.61 (dd, J = 11.4, 6.9 Hz, 1H), 7.53 (t, J = 7.7 Hz, 1H), 6.89 (dd, J = 11.8, 7.2 Hz, 1H). ^{13}C NMR (75 MHz, DMSO-d_6) δ 162.0, 158.3, 155.0, 149.5, 149.2, 149.1, 146.3, 143.3, 135.0, 127.7, 127.2, 126.3, 121.4, 117.8, 117.5, 117.5, 112.5, 112.4, 106.0, 105.6. HR ESI-MS (M + H)$^+$ m/z = 335.0794 (calcd for $C_{14}H_9F_2N_2O_2$: 335.0843).

2-(4-Hydroxy-3,5-dimethoxyphenyl)quinazolin-4(3H)-one (25). Compound **25** (153 mg, quant.) was obtained as a white solid following the procedure of **10**. HPLC purity 95.3% (t_R = 14.06 min). ^{1}H NMR (300 MHz, DMSO-d_6) δ 12.37 (s, 1H), 9.11 (s, 1H), 8.13 (dd, J = 8.0, 1.6

Hz, 1H), 7.86 – 7.77 (m, 1H), 7.71 (d, J = 8.1 Hz, 1H), 7.58 (s, 2H), 7.52 – 7.43 (m, 1H), 3.89 (s,

6H). ^{13}C NMR (75 MHz, DMSO-d_6) δ 162.9, 152.5, 149.3, 148.3, 139.6, 135.0, 127.6, 126.4,

126.3, 122.6, 121.1, 105.9, 56.7. HR ESI-MS (M + Na)$^+$ m/z = 381.1105 (calcd for

$C_{16}H_{14}N_2NaO_4$: 381.1163).

5,7-Dimethoxy-2-(4-(trifluoromethyl)phenyl)quinazolin-4(3H)-one (27). Compound

25 (75 mg, 86%) was obtained as a white solid following the procedure of **10**. HPLC purity

96.6% (t_R = 17.17 min). ^{1}H NMR (300 MHz, DMSO-d_6) δ 12.23 (s, 1H), 8.35 (d, J = 8.2 Hz,

2H), 7.90 (d, J = 8.1 Hz, 2H), 6.79 (s, 1H), 6.58 (s, 1H), 3.88 (d, J = 10.8 Hz, 6H). HR ESI-MS

(M + H)$^+$ m/z = 351.0947 (calcd for $C_{17}H_{14}F_3N_2O_3$: 351.0957).

5,7-Dimethoxy-2-(3-methyl-4-(trifluoromethyl)phenyl)quinazolin-4(3H)-one (28).

Compound **28** (80 mg, 88%) was obtained as a white solid following the procedure of **10**. HPLC

purity 97.5% (t_R = 17.99 min). ^{1}H NMR (300 MHz, DMSO-d_6) δ 12.14 (s, 1H), 8.27 – 8.00 (m,

2H), 7.80 (d, J = 8.3 Hz, 1H), 6.78 (s, 1H), 6.57 (s, 1H), 3.88 (d, J = 11.0 Hz, 6H), 2.52 (s, 3H).

^{13}C NMR (75 MHz, DMSO-d_6) δ 164.8, 161.4, 160.1, 153.0, 152.2, 136.9, 136.4, 131.6, 126.3,

126.0, 101.9, 98.6, 56.5, 56.1, 19.3. HR ESI-MS (M + H)$^+$ m/z = 365.1101 (calcd for

$C_{18}H_{16}F_3N_2O_3$: 365.1113).

2-(4-Hydroxyphenyl)-5,7-dimethoxyquinazolin-4(3H)-one (29). Compound **29** (84 mg,

quant.) was obtained as a yellow solid following the procedure of **10**. HPLC purity 95.4% (t_R =

13.88 min). ^{1}H NMR (300 MHz, DMSO-d_6) δ 11.78 (s, 1H), 10.10 (d, J = 3.3 Hz, 1H), 8.21 –

7.91 (m, 2H), 7.06 – 6.82 (m, 2H), 6.69 (q, J = 2.2 Hz, 1H), 6.48 (q, J = 2.3 Hz, 1H), 4.05 – 3.65

(m, 6H). ^{13}C NMR (75 MHz, DMSO-d_6) δ 164.6, 161.4, 161.0, 160.3, 153.6, 153.2, 129.9, 129.9,

123.3, 115.7, 115.7, 104.9, 101.4, 97.7, 56.4, 56.0. HR ESI-MS (M + H)$^+$ m/z = 299.1021 (calcd

for $C_{16}H_{15}N_2O_4$: 299.1032).

2-(2-Chloro-4-hydroxyphenyl)-5,7-dimethoxyquinazolin-4(3*H*)-one (30). Compound **30** (94 mg, quant.) was obtained as a yellow solid following the procedure of **10**. HPLC purity 97.9% (t_R = 13.82 min). ^{1}H NMR (300 MHz, DMSO-d_6) δ 11.91 (s, 1H), 10.29 (s, 1H), 7.42 (d, *J* = 7.9 Hz, 1H), 6.90 (s, 1H), 6.83 (s, 1H), 6.69 (s, 1H), 6.55 (s, 1H), 3.97 – 3.73 (m, 6H). ^{13}C NMR (75 MHz, DMSO-d_6) δ 164.7, 161.5, 160.0, 159.8, 153.7, 153.3, 132.6, 132.3, 124.8, 116.6, 114.7, 105.3, 101.6, 98.3, 56.5, 56.1. HR ESI-MS $(M + H)^+$ m/z = 333.0630 (calcd for $C_{16}H_{14}ClN_2O_4$: 333.0642).

(*S*)-2-(3,5-Dimethyl-4-(oxiran-2-ylmethoxy)phenyl)-5,7-dimethoxyquinazolin-4(3*H*)-one (31). Compound **31** (215 mg, 94%) was obtained as a white solid following the procedure of **10**. HPLC purity 95.6% (t_R = 17.17 min). ^{1}H NMR (300 MHz, DMSO-d_6) δ 11.80 (s, 1H), 7.88 (s, 2H), 6.72 (d, *J* = 2.2 Hz, 1H), 6.50 (d, *J* = 2.2 Hz, 1H), 5.59 (d, *J* = 3.7 Hz, 1H), 3.86 (d, *J* = 12.2 Hz, 6H), 3.79 (s, 2H), 3.49 (dd, *J* = 10.2, 3.9 Hz, 1H), 3.40 (s, 1H), 2.31 (s, 6H). ^{13}C NMR (75 MHz, DMSO-d_6) δ 164.7, 161.4, 160.2, 158.3, 153.5, 152.9, 131.1, 128.8, 127.9, 105.1, 101.6, 98.0, 75.2, 69.4, 56.4, 56.1, 16.6, 12.1. HR ESI-MS $(M + H)^+$ m/z = 383.1615 (calcd for $C_{21}H_{23}N_2O_5$: 383.1607).

(*S*)-2-(4-(2-Hydroxy-3-(4-methylpiperazin-1-yl)propoxy)-3,5-dimethylphenyl)-5,7-dimethoxyquinazolin-4(3*H*)-one (32). Compound **32** (17 mg, 35%) was obtained as a white solid following the procedure of **39**. HPLC purity 96.1% (t_R = 12.62 min). ^{1}H NMR (300 MHz, MeOD) δ 7.66 (s, 2H), 6.75 (d, *J* = 2.3 Hz, 1H), 6.50 (d, *J* = 2.3 Hz, 1H), 4.14 (dd, *J* = 7.7, 4.5 Hz, 1H), 3.91 (s, 6H), 3.82 (t, *J* = 4.2 Hz, 2H), 2.66 (dd, *J* = 13.3, 8.3 Hz, 10H), 2.35 (d, *J* = 2.8 Hz, 9H). ^{13}C NMR (75 MHz, MeOD) δ 165.4, 161.6, 161.2, 158.6, 153.7, 153., 131.4, 128.1, 127.8, 104.1, 100.3, 97.4, 74.3, 67.6, 60.3, 55.0, 54.8, 54.4, 52.7, 44.4, 15.3. HR ESI-MS (M + Na)$^+$ m/z = 505.2426 (calcd for $C_{26}H_{35}N_4O_5$: 505.2427).

(*E*)-3-(4-(Allyloxy)-3,5-dimethylphenyl)-1-(2-hydroxy-4,6-dimethoxyphenyl)prop-2-en-1-one (36). To a solution of **17** (1,406 mg, 7.4 mmol) and 1-(2-hydroxy-4,6-dimethoxyphenyl)ethan-1-one **35** (1,450 mg, 7.4 mmol) in 20 mL EtOH, 50% KOH (829 mg, 14.8 mmol) was added. After stirring at room temperature overnight, the mixture was concentrated and extracted with CH_2Cl_2. The organic extract was washed with saturated $NaHCO_3$ (aq.), brine and dried over anhydrous Na_2SO_4. The resulting solution was evaporated, and the residue was used directly in the next step.

2-(4-(Allyloxy)-3,5-dimethylphenyl)-5,7-dimethoxy-4*H*-chromen-4-one (37). To a solution of the above residue **36** (1.5 g, 5 mmol) in 10 mL of DMSO, I_2 (130 mg, 0.5 mmol) was added. After stirring at 140 ˚C for 4 h, the mixture was poured into H_2O and extracted with CH_2Cl_2. The organic extract was washed with saturated $NaHCO_3$ (aq.), brine and dried over anhydrous Na_2SO_4. The resulting solution was evaporated, and the residue was purified by silica gel column (CH_2Cl_2/CH_3OH = 50:1) to give the desired product **37** (650 mg, 36%) as a brown foam. HPLC purity 96.4% (t_R = 21.53 min). ^{1}H NMR (300 MHz, CDCl$_3$) δ 7.50 (s, 2H), 6.57 (s, 1H), 6.55 (d, *J* = 2.3 Hz, 1H), 6.34 (d, *J* = 2.2 Hz, 1H), 6.19 – 6.02 (m, 1H), 5.44 (dd, *J* = 17.2, 1.5 Hz, 1H), 5.28 (dd, *J* = 10.4, 1.2 Hz, 1H), 4.35 (d, *J* = 5.6 Hz, 2H), 3.91 (d, *J* = 9.8 Hz, 6H), 2.34 (s, 6H). ^{13}C NMR (75 MHz, CDCl$_3$) δ 177.6, 163.9, 160.8, 160.7, 159.9, 158.6, 133.6, 131.8, 126.8, 126.6, 117.6, 109.2, 108.4, 96.1, 92.8, 73.2, 56.3, 55.7, 16.6. MS (M + H)$^+$ m/z 367.2. HR ESI-MS (M + H)$^+$ m/z = 367.1548 (calcd for $C_{22}H_{23}O_5$: 367.1545)

2-(4-Hydroxy-3,5-dimethylphenyl)-5,7-dimethoxy-4*H*-chromen-4-one (38). To a solution of **35** (630 mg, 1.72 mmol) in 10 mL of CH_3OH, Pd(PPh$_3$)$_4$ (60 mg, 0.05 mmol) and K_2CO_3 (949 mg, 6.88 mmol) were added. After stirring at 90 ˚C for 7 h, the mixture was poured into 1 N HCl and extracted with *n*-BuOH. The organic extract was concentrated and CH_2Cl_2 was

added to precipitate. The precipitate was filtered to get **36** (420 mg, 75%) as a yellow solid. HPLC purity 97.4% (t_R = 17.96 min). ^{1}H NMR (300 MHz, DMSO-d_6) δ 7.64 (s, 2H), 6.86 (d, J = 2.1 Hz, 1H), 6.57 (s, 1H), 6.49 (d, J = 2.1 Hz, 1H), 3.90 (s, 3H), 3.82 (s, 3H), 2.25 (s, 6H). ^{13}C NMR (75 MHz, DMSO-d_6) δ 176.2, 164.0, 160.9, 160.6, 159.6, 157.1, 126.7, 125.3, 121.6, 108.7, 106.6, 96.7, 93.8, 56.6, 49.0, 17.2. MS (M + H)[+] m/z 327.1. HR ESI-MS (M + H)[+] m/z = 327.1234 (calcd for $C_{19}H_{19}O_5$: 327.1232).

2-(4-(2-Hydroxyethoxy)-3,5-dimethylphenyl)-5,7-dimethoxy-4*H*-chromen-4-one (39). To a solution of **38** (20 mg, 0.061 mmol) in 5 mL of DMF, K_2CO_3 (25 mg, 0.184 mmol) and 2-bromoethanol (15 mg, 0.123 mmol) were added. The mixture was allowed to heat at 80 ˚C overnight. Then the mixture was poured into water and extracted by CH_2Cl_2. The organic extract was washed with saturated $NaHCO_3$ (aq.), brine and dried over anhydrous Na_2SO_4. The resulting solution was evaporated, and the residue was purified by silica gel column (CH_2Cl_2/CH_3OH = 20:1) to give the desired product **39** (12 mg, 55%) as a white solid. ^{1}H NMR (300 MHz, Chloroform-*d*) δ 7.53 (s, 2H), 6.58 (d, J = 5.8 Hz, 2H), 6.38 (s, 1H), 3.96 (t, J = 10.0 Hz, 10H), 2.37 (s, 7H). ^{13}C NMR (75 MHz, CDCl$_3$) δ 177.6, 164.0, 160.9, 160.6, 159.9, 158.1, 131.6, 127.0, 126.7, 109.2, 108.5, 96.1, 92.8, 73.3, 62.2, 56.4, 55.8, 16.5. MS (M + H)[+] m/z 371.1. HR ESI-MS (M + H)[+] m/z = 371.1483 (calcd for $C_{21}H_{23}O_6$: 371.1495).

(*S*)-2-(3,5-Dimethyl-4-(oxiran-2-ylmethoxy)phenyl)-5,7-dimethoxy-4*H*-chromen-4-one (40). Compound **40** (420 mg, 72%) was obtained as a white solid following the procedure of **39**. ^{1}H NMR (300 MHz, CDCl$_3$) δ 7.54 (s, 2H), 6.59 (d, J = 3.6 Hz, 2H), 6.38 (d, J = 2.3 Hz, 1H), 4.13 (dd, J = 11.2, 3.0 Hz, 1H), 3.94 (d, J = 10.6 Hz, 6H), 3.79 (dd, J = 11.1, 6.1 Hz, 1H), 3.39 (q, J = 3.3 Hz, 1H), 2.92 (t, J = 4.6 Hz, 1H), 2.74 (dd, J = 5.0, 2.6 Hz, 1H), 2.38 (s, 6H). [13]C

NMR (75 MHz, CDCl₃) δ 177.5, 163.9, 160.9, 160.5, 159.9, 158.2, 131.6, 127.2, 126.7, 109.3, 108.6, 96.1, 92.8, 77.2, 73.3, 56.4, 55.7, 50.4, 44.5, 16.5.

(*R*)-2-(3,5-Dimethyl-4-(oxiran-2-ylmethoxy)phenyl)-5,7-dimethoxy-4*H*-chromen-4-one (41). To a solution of **38** (100 mg, 0.31 mmol) in 5 mL acetone, (*R*)-(-)-epichlorohydrin (285 mg, 3.1 mmol) and K₂CO₃ (211 mg, 1.53 mmol) were added. The mixture was refluxed for 24 h and then poured into H₂O. The solution was extracted with CH₂Cl₂ (20 mL × 3). The organic layer was washed with saturated NaHCO₃ (aq.), brine and dried over anhydrous Na₂SO₄. The resulting solution was filtered and concentrated to give a crude solid, which was used directly in the next step without further purifications.

(*S*)-2-(4-(2-Hydroxy-3-(piperidin-1-yl)propoxy)-3,5-dimethylphenyl)-5,7-dimethoxy-4*H*-chromen-4-one (42). Compound **42** (55 mg, 44%) was obtained as a white solid following the procedure of **39**. HPLC purity 98.2% (t_R = 16.17 min). ¹H NMR (300 MHz, DMSO-d_6) δ 7.68 (s, 2H), 6.81 (s, 1H), 6.62 (s, 1H), 6.47 (s, 1H), 4.83 (s, 1H), 3.95 (d, *J* = 5.2 Hz, 1H), 3.89 (s, 3H), 3.82 (s, 3H), 3.79 – 3.69 (m, 2H), 2.42 (tt, *J* = 13.8, 8.3 Hz, 6H), 2.31 (s, 6H), 1.48 (q, *J* = 5.5 Hz, 4H), 1.37 (d, *J* = 6.1 Hz, 2H). ¹³C NMR (75 MHz, DMSO-d_6) δ 176.0, 164.1, 160.7, 160.1, 159.6, 158.7, 131.8, 126.9, 126.3, 108.8, 107.9, 96.7, 93.7, 75.4, 67.6, 61.8, 56.48, 56.4, 55.2, 26.1, 24.4, 16.5. HR ESI-MS (M + H)⁺ m/z = 468.2392 (calcd for C₂₇H₃₄NO₆: 468.2390).

(*S*)-2-(4-(2-hydroxy-3-(4-methylpiperazin-1-yl)propoxy)-3,5-dimethylphenyl)-5,7-dimethoxy-4*H*-chromen-4-one (43). Compound **43** (32 mg, 24%) was obtained as a white solid following the procedure of **39**. HPLC purity 98.6% (t_R = 14.01 min). ¹H NMR (300 MHz, DMSO-d_6) δ 7.69 (s, 2H), 6.83 (d, *J* = 2.2 Hz, 1H), 6.63 (s, 1H), 6.53 – 6.42 (m, 1H), 4.55 (s, 1H), 3.98 – 3.93 (m, 1H), 3.89 (s, 3H), 3.82 (s, 3H), 3.76 (dd, *J* = 9.2, 4.5 Hz, 2H), 2.53 (s, 1H), 2.38 (d, *J* = 43.1 Hz, 15H), 2.13 (s, 3H). ¹³C NMR (75 MHz, DMSO-d_6) δ 176.0, 164.1, 160.7,

160.1, 159.6, 158.7, 131.9, 126.9, 126.3, 108.8, 108.0, 96.7, 93.7, 75.3, 74.3, 67.7, 61.0, 56.5, 56.4, 55.3, 53.8, 46.2, 16.5. HR ESI-MS (M + H)$^+$ m/z = 483.2493 (calcd for $C_{27}H_{35}N_2O_6$: 483.2495).

(*R*)-2-(4-(2-Hydroxy-3-(piperidin-1-yl)propoxy)-3,5-dimethylphenyl)-5,7-dimethoxy-4*H*-chromen-4-one (44). To a solution of **41** (48 mg, 0.164 mmol) in 2 mL of EtOH and 2 mL of DMF, piperidine (139 mg, 1.64 mmol) and K_2CO_3 (226 mg, 1.64 mmol) were added. The mixture was refluxed for 24 h and then poured into H_2O. The solution was extracted with CH_2Cl_2 (20 mL × 3). The organic layer was washed with saturated $NaHCO_3$ (aq.), brine and dried over anhydrous Na_2SO_4. The resulting solution was filtered and concentrated to give a solid residue. The crude product was purified by PTLC (CH_2Cl_2:CH_3OH = 20:1) to give **44** (13 mg, 18% for two steps) as a white solid. HPLC purity 98.6% (t_R = 16.8 min). ^{1}H NMR (300 MHz, MeOD) δ 7.50 (s, 2H), 6.63 (s, 1H), 6.44 (d, *J* = 21.6 Hz, 2H), 4.00 – 3.77 (m, 9H), 2.73 (s, 6H), 2.32 (s, 6H), 1.63 (d, *J* = 43.9 Hz, 6H). ^{13}C NMR (75 MHz, MeOD) δ 178.4, 164.9, 161.5, 160.5, 159.8, 158.5, 131.7, 126.5, 126.2, 107.8, 106.6, 95.9, 92.7, 74.4, 66.9, 61.0, 55.2, 54.6, 24.8, 23.3, 15.3. HR ESI-MS (M + H)$^+$ m/z = 468.2390 (calcd for $C_{27}H_{34}NO_6$: 468.2386).

(*R*)-2-(4-(2-Hydroxy-3-(4-methylpiperazin-1-yl)propoxy)-3,5-dimethylphenyl)-5,7-dimethoxy-4*H*-chromen-4-one (45). To a solution of **41** (48 mg, 0.164 mmol) in 5 mL of DMF, 1-methylpiperazine (164 mg, 1.64 mmol) and K_2CO_3 (226 mg, 1.64 mmol) were added. The mixture was refluxed for 24 h and then poured into H_2O. The solution was extracted with CH_2Cl_2 (20 mL × 3). The organic layer was washed with saturated $NaHCO_3$ (aq.), brine and dried over anhydrous Na_2SO_4. The resulting solution was filtered and concentrated to give a crude solid. The crude product was purified by PTLC (CH_2Cl_2:CH_3OH = 20:1) to give **45** (16 mg, 20% for two steps) as a white solid. HPLC purity 96.8% (t_R = 14.8 min). ^{1}H NMR (300 MHz, CDCl$_3$) δ

7.45 (s, 2H), 6.49 (d, J = 6.4 Hz, 2H), 6.29 (s, 1H), 4.02 (s, 1H), 3.82 (s, 8H), 2.49 (dd, J = 39.7, 24.1 Hz, 10H), 2.25 (d, J = 6.1 Hz, 9H). ^{13}C NMR (75 MHz, CDCl$_3$) δ 182.,5 168.4, 165.4, 164.7, 163.9 162.3, 135.7, 130.8, 112.6, 111.7, 100.2, 96.8, 78.1, 70.6, 64.3, 59.9, 59.7, 58.6, 56.6, 49.3, 20.2. MS (M + H)$^+$ m/z 483.2. HR ESI-MS (M + H)$^+$ m/z = 483.2482 (calcd for C$_{27}$H$_{35}$N$_2$O$_6$: 483.2495).

(R)-2-(4-(2-Hydroxy-3-morpholinopropoxy)-3,5-dimethylphenyl)-5,7-dimethoxy-4H-chromen-4-one (46). Compound **46** (76 mg, 65%) was obtained as a white solid following the procedure of **42.** HPLC purity 95.6% (t_R = 15.30 min). ^{1}H NMR (300 MHz, MeOD) δ 7.42 (d, J = 3.3 Hz, 2H), 6.55 (d, J = 2.3 Hz, 1H), 6.41 (s, 1H), 6.34 (d, J = 2.4 Hz, 1H), 4.14 (dd, J = 7.7, 4.6 Hz, 1H), 3.88 (s, 3H), 3.84 (s, 3H), 3.80 (dd, J = 4.8, 3.0 Hz, 2H), 3.74 (t, J = 4.7 Hz, 3H), 3.67 (t, J = 4.8 Hz, 1H), 3.33 (t, J = 1.7 Hz, 1H), 2.61 (td, J = 8.5, 7.7, 4.0 Hz, 5H), 2.29 (s, 6H). ^{13}C NMR (75 MHz, MeOD) δ 178.3, 164.7, 161.3, 160.4, 159.6, 158.5, 131.6, 126.3, 126.0, 107.8, 106.5, 95.8, 92.6, 74.3, 67.4, 66.5, 61.0, 55.1, 55.0, 54.0, 15.3. HR ESI-MS (M + H)$^+$ m/z = 470.2187 (calcd for C$_{26}$H$_{32}$NO$_7$: 470.2179).

(R)-2-(4-(3-(4,4-Difluoropiperidin-1-yl)-2-hydroxypropoxy)-3,5-dimethylphenyl)-5,7-dimethoxy-4H-chromen-4-one (47). Compound **47** (75 mg, 60%) was obtained as a white solid following the procedure of **42.** HPLC purity 97.6% (t_R = 16.00 min). ^{1}H NMR (300 MHz, CDCl$_3$) δ 7.51 (s, 2H), 6.60 – 6.52 (m, 2H), 6.35 (d, J = 2.3 Hz, 1H), 4.10 (dd, J = 8.9, 4.6 Hz, 1H), 3.92 (d, J = 9.6 Hz, 6H), 3.84 (d, J = 5.6 Hz, 2H), 2.85 – 2.75 (m, 2H), 2.65 (td, J = 8.5, 5.6 Hz, 4H), 2.35 (s, 6H), 2.12 – 1.95 (m, 4H). ^{13}C NMR (75 MHz, CDCl$_3$) δ 177.5, 163.9, 160.8, 160.5, 159.8, 158.1, 131.6, 127.0, 126.7, 124.8, 121.6, 118.4, 109.2, 108.4, 96.1, 92.8, 77.3, 74.1, 66.8, 59.5, 56.4, 55.7, 50.4, 50.4, 50.3, 34.4, 34.0, 33.7, 16.5. HR ESI-MS (M + H)$^+$ m/z = 504.2189 (calcd for C$_{27}$H$_{32}$F$_2$NO$_6$: 504.2198).

(*R*)-2-(4-(2-Hydroxy-3-(pyrrolidin-1-yl)propoxy)-3,5-dimethylphenyl)-5,7-

dimethoxy-4*H*-chromen-4-one (48). Compound **48** (30 mg, 27%) was obtained as a white solid

following the procedure of **42.** HPLC purity 99.2% (t_R = 15.85 min). ^{1}H NMR (300 MHz, MeOD)

δ 7.49 (s, 2H), 6.62 (d, *J* = 2.3 Hz, 1H), 6.47 (s, 1H), 6.39 (d, *J* = 2.3 Hz, 1H), 4.15 (dd, *J* = 8.8,

4.5 Hz, 1H), 3.97 – 3.75 (m, 9H), 2.88 (dd, *J* = 12.6, 4.2 Hz, 1H), 2.74 (t, *J* = 6.2 Hz, 4H), 2.32

(s, 6H), 1.86 (p, *J* = 3.1 Hz, 4H). ^{13}C NMR (75 MHz, MeOD) δ 178.3, 164.8, 161.4, 160.5, 159.7,

158.6, 131.6, 126.4, 126.1, 107.8, 106.6, 95.9, 92.7, 74.5, 68.9, 58.7, 55.11, 55.06, 54.3, 22.9,

15.3. HR ESI-MS (M + H)[+] m/z = 454.2223 (calcd for $C_{26}H_{32}NO_6$: 454.2230).

(*R*)-2-(4-(3-(Dimethylamino)-2-hydroxypropoxy)-3,5-dimethylphenyl)-5,7-

dimethoxy-4*H*-chromen-4-one (49). Compound **49** (20 mg, 38%) was obtained as a white solid

following the procedure of **42.** HPLC purity 95.8% (t_R = 15.67 min). ^{1}H NMR (300 MHz,

DMSO-d_6) δ 7.72 (s, 2H), 6.86 (d, *J* = 2.3 Hz, 1H), 6.65 (s, 1H), 6.50 (d, *J* = 2.3 Hz, 1H), 4.97 (d,

J = 4.7 Hz, 1H), 4.66 (t, *J* = 5.5 Hz, 1H), 4.12 (q, *J* = 5.1 Hz, 1H), 3.90 (s, 3H), 3.83 (s, 3H), 3.80

– 3.68 (m, 2H), 3.56 – 3.44 (m, 6H), 3.17 (d, *J* = 5.0 Hz, 1H), 2.32 (s, 6H). ^{13}C NMR (75 MHz,

DMSO-d_6) δ 176.1, 164.2, 160.7, 160.2, 159.7, 158.9, 131.9, 127.0, 126.3, 108.8, 108.0, 96.8,

93.8, 74.4, 71.2, 63.1, 56.5, 56.5, 49.1, 46.4, 16.6. HR ESI-MS (M + H)[+] m/z = 428.2064 (calcd

for $C_{24}H_{30}NO_6$: 428.2073).

(*S*)-2-(4-(2-fluoro-3-(piperidin-1-yl)propoxy)-3,5-dimethylphenyl)-5,7-dimethoxy-4*H*-

chromen-4-one (50). To a solution of **44** (10 mg, 0.021 mmol) in 1 mL CH_2Cl_2, DAST (5.2 mg,

0.032 mmol) was added. The mixture was allowed to stir at room temperature overnight and then

concentrated. The residue was purified by PTLC and **50** (8 mg, 80%) was obtained as a white

solid. HPLC purity 95.9% (t_R = 16.99 min). ^{1}H NMR (300 MHz, CDCl₃) δ 7.55 (s, 2H), 6.67 –

6.52 (m, 2H), 6.39 (d, *J* = 2.3 Hz, 1H), 4.91 (d, *J* = 4.5 Hz, 1H), 4.76 (d, *J* = 4.6 Hz, 1H), 3.95 (d,

J = 10.8 Hz, 8H), 3.22 – 3.03 (m, 1H), 2.73 (d, *J* = 4.7 Hz, 4H), 2.38 (s, 6H), 1.60 (d, *J* = 6.3 Hz, 4H), 1.49 (d, *J* = 5.7 Hz, 2H). ^{13}C NMR (75 MHz, CDCl$_3$) *δ* 177.55, 163.9, 160.9, 160.6, 159.9, 158.4, 131.7, 127.0, 126.7, 109.3, 108.5, 96.1, 92.8, 82.6, 80.4, 68.9, 68.9, 64.5, 64.3, 56.4, 55.7, 51.6, 26.6, 24.6, 16.6. HR ESI-MS (M + H)$^+$ m/z = 470.2330 (calcd for C27H33FNO5: 470.2343).

Crystollagraphy. Crystals of human BRD4 BD1 in complex with the ligand compound **45** were prepared *via* hanging drop vapor diffusion at 20 °C. 10 mg/mL human BRD4 BD1 protein solution with 2 mM compound **45** was pre-incubated on ice for 10 min prior to being mixed in 1:1 ratio (protein: reservoir solution) with 100 mM HEPES and 15% (w/v) PEG 3350 at pH 7.5. Orthorhombic crystals grew within 3 days and were subsequently cryoprotected with 100 mM HEPES and 30% (w/v) PEG 3350 at pH 7.5 containing 2 mM compound **45**. X-ray diffraction data were collected at beamline 22-ID at the Advanced Photon Source (Argonne National Labs). The diffraction data was processed and integrated using the iMOSFLM v7.2.2,[30] AIMLESS and CTRUNCATE[31] programs were used for scaling and anisotropy correction respectively. The phase information was obtained by molecular replacement using a single chain of human BRD4 BD structure (PDB 5KU3) as a search model. Iterative cycles of manual model building and refinement were performed within Phenix v1.16-3549[32] and COOT v0.8.9.1[33] software.

Determination of Aqueous Solubility. Solubility in water for **44** and **45** was determined by HPLC analysis according to a previously published protocol.[34, 35] First, 1~2 mgs of **44** and **45** were weighed and added to 1 mL of water, respectively. Then, 10-15 mgs of **44** and **45** were weighed and added to 0.1-0.6 mL of water. The suspensions were shaken at 25 °C for 24 h and then centrifuged, and the supernatants were filtered. Aliquots (5 µL) of the supernatants were

injected into the HPLC system equipped with a C18 reverse-phase column under the same

condition which was described in the general Experimental Section. One-point calibration[36] was

done by injecting 5 μL aliquots of the corresponding buffer solutions of **44** or **45** with known

concentrations.

Cell Culture. Immortalized hSAECs were previously described.[37, 38] hSAECs were grown

in SAGM small airway epithelial cell growth medium (Lonza, Walkersville, MD) in a

humidified atmosphere of 5% CO_2. Poly(I:C) was obtained from Sigma (St. Louis, MO) and

used at 10 µg/mL in cell culture. Compound **1** was purchased from Tocris and compound **3** was

either purchased from Cayman Chemical (Ann Arbor, Michigan) or resynthesized in house.

Compounds were dissolved in DMSO and added at the indicated concentrations.

Quantitative Real-Time PCR (Q-RT-PCR). For gene expression analyses, 1 µg of RNA

was reverse transcribed using Super Script III as previously described. One µL of cDNA product

was amplified using SYBR Green Supermix (Bio-Rad) and indicated gene-specific primers. The

reaction mixtures were subjected to 40 cycles of 15 s at 94 ˚C, 60 s at 60 ˚C, and 1 min at 72 ˚C

in an iCycler (BioRad). Quantification of relative changes in gene expression was calculated

using the ΔΔCt method and expression as the fold change between experimental and control

samples was normalized to internal control cyclophilin (PPIA).[39]

***In Vitro* Efficacy of BRD4 Inhibitors on Poly(I:C)-Induced Innate Immune Response.**

hSAECs were first pretreated with a series of final concentrations of BRD4 inhibitors from 0.01

nM to 100 µM for 24 h and were then added poly(I:C) at 10 µg/mL for another 4 h prior to

harvesting the cells. The harvested cells were first washed with PBS twice and then the total

RNA was extracted using acid guanidinium phenol extraction (Tri Reagent; Sigma). The total

RNA was further reverse-transcribed for gene expression analysis by Q-RT-PCR. The inhibitory

effect of BRD4 inhibitors on poly(I:C)-induced innate immune gene expression was compared with that of poly(I:C) alone and inhibitory percentage of each treatment was obtained.[8] For compounds **1**, **3**, **32**, **34**, **39**, **42~45** and **48**, *in vitro* efficacy of these BRD4 inhibitors on poly(I:C) induced innate immune response were presented as the IC_{50} values of these compounds. Compounds were dissolved in DMSO and further diluted at cell culture medium to appropriate concentrations.

Time-Resolved Fluorescence Energy Transfer (TR-FRET) Assays. 384 well plate-based commercial TR-FRET Assay kits (Cayman Chemical, Ann Arbor, Michigan) were used to determine the binding ability of tested BRD4 inhibitors to the BRD4 and BRD2 BDs (BD) using the two recombinant BRD4 BDs or BRD2 BDs by TR-FRET assays. A series of concentrations of BRD4 inhibitors from 0.01 nM to 100 μM were added into a 384 well test plate and mixed with other reaction components based on the instructions from vendor followed by incubation 1 h at room temperature. The commercially available BRD inhibitors compounds **1** and **3** were used as the controls. The plates were read in time-resolved format by exciting the sample at 340 nm and reading emissions at 620 and 670 nm, using a 100 μs delay and a 500 μs window at a Tecan M1000 pro reader. A plot of the TR-FRET ratio (670 nm emission/620 nm emission versus inhibitor concentration on semi-log axes results in a sigmoidal dose-response curve typical of competitive assays. These data were further calculated out with the IC_{50} values of tested BRD4 inhibitors to the BDs of BRD2 and BRD4 as well as other relevant target proteins, respectively.[8, 12]

In Vivo **Efficacy of BRD4 Inhibitors on Poly(I:C)-Induced Acute Airway Inflammation.** Animal experiments were performed according to the NIH Guide for Care and Use of Experimental Animals and approved by the University of Texas Medical Branch (UTMB)

Animal Care and Use Committee (approval no. 1312058A). Male C57BL6/J mice (12 weeks old) were purchased from The Jackson Laboratory (Bar Harbor, ME) and housed under pathogen-free conditions with food and water ad libitum. C57BL/6 mice were pre-treated in the absence or presence of the indicated BRD4 inhibitors (10 mg/kg body weight, via the intraperitoneal route) one day prior to poly(I:C) stimulation. The next day, animals (5 mice per group) were given another dose of BRD4 inhibitor immediately followed by intranasal (i.n.) administration of phosphate-buffered saline (PBS, 50 µL) or poly(I:C) (300 µg dissolved in 50 µL PBS). One day later, the mice were euthanized. The bronchoalveolar lavage fluid (BALF) and lung tissues of treated mice were collected for further analysis. Compounds were first dissolved in DMSO and further diluted in 10% hydroxypropyl β-cyclodextrin in PBS to appropriate concentration prior to intraperitoneal administration.[8, 12]

Evaluation of Airway Inflammation. Cellular recruitment into the airway lumen was assessed in the BALF. Lungs were perfused twice with 1 mL of sterile PBS (pH 7.4) to obtain the BALF. Total cell counts were determined by trypan blue staining 50 μL of BALF and counting viable cells using a hemocytometer. Differential cell counts were performed on cytocentrifuge preparations (Cytospin 3; Thermo Shandon, Pittsburgh, Pa) stained with Wright-Giemsa. A total of 300 cells were counted per sample using light microscopy. Formalin-fixed lungs were embedded in paraffin, sectioned at a 4 μm thickness, and stained with hematoxylin and eosin or Masson's trichrome. Microscopy was performed on a NIKON Eclipse Ti System.[8, 12]

Cytokine Bio-Plex Assay. BALF samples were centrifuged (800 x g for 5 min at 4 °C) and the cytokines quantitated in the supernatant using the Bio-Plex Pro™ Mouse Cytokine Assay (Bio-Rad, Hercules, CA) with recombinant cytokine standards (in triplicate). Readings were

performed on a Bioplex® 200™ system (Bio-Rad). Data was analyzed using Bio-Plex Manager™ Software Version 6.0 Build 617 (Bio-Rad).[8, 12]

Immunofluorescence Confocal Microscopy (IFCM). Cultured hSAECs were plated on rat tail collagen-treated cover glasses. Afterwards, the cells were first preincubated with compound **44** or **45** at final concentration of 10 μM for 24 h and were then added poly(I:C) at 10 µg/mL for another 4 h prior to harvesting the cells. The cells were fixed with 4% paraformaldehyde in PBS and incubated with 0.1 M ammonium chloride for 10 min. Cells were permeabilized with 0.5% Triton-100, followed by incubation in blocking buffer (5% goat serum, 0.1% IGEPAL CA-630, 0.05% NaN$_3$, and 1% BSA) and incubated with anti-H3K122Ac (Abcam, Cambridge, MA) in incubation buffer (0.1% IGEPAL CA-630, 0.05% NaN$_3$, and 2% BSA) overnight at 4 °C. After washing, cells were stained with Alexa Fluor 488-conjugated goat anti-rabbit IgG (Life Technologies, Carlsbad, CA), respectively, in incubation buffer for 1 h, then counterstained with nuclear marker DAPI (Sigma-Aldrich, St. Louis, MO) and visualized with a Nikon fluorescence confocal microscope, magnification 63 ×.[10, 12]

Formalin-fixed, paraffin-embedded lung sections were rehydrated using serial concentrations of ethanol. Antigen retrieval was performed with antigen unmasking solution based on recommendations from Abcam (TE buffer, pH 9.0). Paraffin-embedded sections were blocked using 0.1% Triton-X, 5% normal goat serum and incubated with rabbit anti-acetyl H3K122 Ab (Abcam, Cambridge, MA) overnight at 4 °C. Normal anti-rabbit IgG was used as staining specificity controls. After washing, cells were stained with Alexa Fluor 568-conjugated goat anti-rabbit IgG (Life Technologies) in incubation buffer for 1 h, then counterstained with nuclear marker DAPI (Sigma-Aldrich, St. Louis, MO) and visualized with a LSM510 fluorescence confocal microscope, magnification 63 ×.[10,12]

ASSOCIATED CONTENT

Supporting Information

The Supporting Information is available free of charge at http://pubs.acs.org.

Co-complex crystal structures of **45** with human BRD4 BD1 protein; superimposition of BRD4 BD1 with BRD3 BD1; Plasma concentration curves of compound **45** in male SD rats after IV and PO administration; BROMO*scan*™ profiling of compound **45**; Target panel assays by NIMH/NIH psychoactive drug screening program (PDSP) for compound **45**; data collection and refinement statistics for the crystal analysis of BRD4 inhibitor **45** co-complexed with human BRD4 BD1; representative HPLC analysis; copies of ^{1}H and ^{13}C NMR spectra of all new compounds (PDF)

Molecular formula strings and some data (CSV)

Accession Codes

PDB code for BRD4 BD1 protein co-complexed with **45** is 6UWU. Authors will release the atomic coordinates and experimental data upon article publication.

AUTHOR INFORMATION

Corresponding Author

For J.Z.: phone, (409) 772-9748; fax, (409) 772-9648; e-mail, jizhou@utmb.edu.

For B.T.: phone, (409) 772-1177; fax, (409) 772-8709; e-mail, bitian@utmb.edu.

For A.R.B.: phone, (608) 263-7371; email, abrasier@wisc.edu.

Notes

The authors declare no competing financial interest.

ABBREVIATIONS USED

KAc, lysine acetylation; HATs, histone acetyl transferases; HDAC, histone deacetylase; BET, bromodomain and extra terminal domain; BRD4, bromodomain-containing protein 4; MACE, major adverse cardiovascular events; TLR3, toll-like receptor 3; hSAECs, human small airway epithelial cells; PK, pharmacokinetic; WPF, tryptophan-proline-phenylalanine; THF, tetrahydrofuran; DIPEA, *N,N*-diisopropylethylamine; NaH, sodium hydride; Pd(PPh$_3$)$_4$, tetrakis(triphenylphosphin)palladium; DAST, diethylaminosulfur trifluoride; qRT-PCR, quantitative real-time PCR; TR-FRET, time-resolved fluorescence energy transfer; i.v., intravenously; p.o., per os; MLM, mouse liver microsomes; HLM, human liver microsomes; t$_{1/2}$,

half-life; C_{max}, maximum plasma concentration; AUC_{0-t}, total exposure following single dose; V_{SS}, volume of distribution at steady state; CL, total clearance; *F*, oral bioavailability; p.o., oral administration; i.p., intraperitoneal administration; i.n., intranasal; BALF, bronchoalveolar lavage fluid; SAR, structure-activity relationship; IFCM, Immunofluorescence confocal microscopy.

REFERENCES

1.   Berdasco, M.; Esteller, M. Clinical Epigenetics: Seizing Opportunities for Translation. *Nat. Rev. Genet.* **2019,** 20, 109-127.

2.   Rakyan, V. K.; Down, T. A.; Balding, D. J.; Beck, S. Epigenome-wide Association Studies for Common Human Diseases. *Nat. Rev. Genet.* **2011,** 12, 529-541.

3.   Kuo, M. H.; Allis, C. D. Roles of Histone Acetyltransferases and Deacetylases in Gene Regulation. *Bioessays* **1998,** 20, 615-626.

4.   Liu, Z.; Wang, P.; Chen, H.; Wold, E. A.; Tian, B.; Brasier, A. R.; Zhou, J. Drug Discovery Targeting Bromodomain-Containing Protein 4. *J. Med. Chem.* **2017,** 60, 4533-4558.

5.   Filippakopoulos, P.; Knapp, S. Targeting Bromodomains: Epigenetic Readers of Lysine Acetylation. *Nat. Rev. Drug Discov.* **2014,** 13, 337-356.

6.   Cochran, A. G.; Conery, A. R.; Sims, R. J., 3rd. Bromodomains: a New Target Class for Drug Development. *Nat. Rev. Drug Discov.* **2019,** 18, 609-628.

7.   Belkina, A. C.; Denis, G. V. BET Domain Co-regulators in Obesity, Inflammation and Cancer. *Nat. Rev. Cancer* **2012,** 12, 465-477.

8.   Liu, Z.; Tian, B.; Chen, H.; Wang, P.; Brasier, A. R.; Zhou, J. Discovery of Potent and Selective BRD4 Inhibitors Capable of Blocking TLR3-Induced Acute Airway Inflammation. *Eur. J. Med. Chem.* **2018,** 151, 450-461.

9.   Zhao, Y.; Tian, B.; Sun, H.; Zhang, J.; Zhang, Y.; Ivannikov, M.; Motamedi, M.; Liu, Z.; Zhou, J.; Kaphalia, L.; Calhoun, W. J.; Maroto, R.; Brasier, A. R. Pharmacoproteomics Reveal Novel Protective Activity of Bromodomain Containing 4 Inhibitors on Vascular Homeostasis in TLR3-Mediated Airway Remodeling. *J. Proteomics* **2019,** 205, 103415.

10.   Tian, B.; Hosoki, K.; Liu, Z.; Yang, J.; Zhao, Y.; Sun, H.; Zhou, J.; Rytting, E.; Kaphalia, L.; Calhoun, W. J.; Sur, S.; Brasier, A. R. Mucosal Bromodomain-Containing Protein 4 Mediates Aeroallergen-Induced Inflammation and Remodeling. *J. Allergy Clin. Immun.* **2019,** 143, 1380-1394.

11.   Nicodeme, E.; Jeffrey, K. L.; Schaefer, U.; Beinke, S.; Dewell, S.; Chung, C. W.; Chandwani, R.; Marazzi, I.; Wilson, P.; Coste, H.; White, J.; Kirilovsky, J.; Rice, C. M.; Lora, J. M.; Prinjha, R. K.; Lee, K.; Tarakhovsky, A. Suppression of Inflammation by a Synthetic Histone Mimic. *Nature* **2010,** 468, 1119-1123.

12.   Tian, B.; Liu, Z.; Yang, J.; Sun, H.; Zhao, Y.; Wakamiya, M.; Chen, H.; Rytting, E.; Zhou, J.; Brasier, A. R. Selective Antagonists of the Bronchiolar Epithelial NF-kB-Bromodomain-Containing Protein 4 Pathway in Viral-Induced Airway Inflammation. *Cell Rep.* **2018,** 23, 1138-1151.

13.   Tian, B.; Liu, Z.; Litvinov, J.; Maroto, R.; Jamaluddin, M.; Rytting, E.; Patrikeev, I.; Ochoa, L.; Vargas, G.; Motamedi, M.; Ameredes, B. T.; Zhou, J.; Brasier, A. R. Efficacy of Novel Highly Specific Bromodomain-Containing Protein 4 Inhibitors in Innate Inflammation-Driven Airway Remodeling. *Am. J. Respir. Cell Mol. Biol.* **2019,** 60, 68-83.

14.   Brasier, A. R.; Zhou, J. Validation of the Epigenetic Reader Bromodomain-Containing Protein 4 (BRD4) as a Therapeutic Target for Treatment of Airway Remodeling. *Drug Discov. Today* **2019,** 25, 126-132.

15.   Li, Z.; Guo, J.; Wu, Y.; Zhou, Q. The BET Bromodomain Inhibitor JQ1 Activates HIV Latency Through Antagonizing BRD4 Inhibition of Tat-Transactivation. *Nucleic Acids Res.* **2013,** 41, 277-287.

16.   Niu, Q.; Liu, Z.; Alamer, E.; Fan, X.; Chen, H.; Endsley, J.; Gelman, B. B.; Tian, B.; Kim, J. H.; Michael, N. L.; Robb, M. L.; Ananworanich, J.; Zhou, J.; Hu, H. Structure-Guided Drug Design Identifies a BRD4-Selective Small Molecule That Suppresses HIV. *J. Clin. Invest.* **2019,** 129, 3361-3373.

17.   Zhu, J.; Gaiha, G. D.; John, S. P.; Pertel, T.; Chin, C. R.; Gao, G.; Qu, H.; Walker, B. D.; Elledge, S. J.; Brass, A. L. Reactivation of Latent HIV-1 by Inhibition of BRD4. *Cell Rep.* **2012,** 2, 807-816.

18.   Duan, Q.; McMahon, S.; Anand, P.; Shah, H.; Thomas, S.; Salunga, H. T.; Huang, Y.; Zhang, R.; Sahadevan, A.; Lemieux, M. E.; Brown, J. D.; Srivastava, D.; Bradner, J. E.; McKinsey, T. A.; Haldar, S. M. BET Bromodomain Inhibition Suppresses Innate Inflammatory and Profibrotic Transcriptional Networks in Heart Failure. *Sci. Transl. Med.* **2017,** 9, pii: eaah5084.

19.   Korb, E.; Herre, M.; Zucker-Scharff, I.; Darnell, R. B.; Allis, C. D. BET Protein BRD4 Activates Transcription in Neurons and BET Inhibitor JQ1 Blocks Memory in Mice. *Nat. Neurosci.* **2015,** 18, 1464-1473.

20.   Zhang, G.; Smith, S. G.; Zhou, M. M. Discovery of Chemical Inhibitors of Human Bromodomains. *Chem. Rev.* **2015,** 115, 11625-11668.

21.   Filippakopoulos, P.; Qi, J.; Picaud, S.; Shen, Y.; Smith, W. B.; Fedorov, O.; Morse, E. M.; Keates, T.; Hickman, T. T.; Felletar, I.; Philpott, M.; Munro, S.; McKeown, M. R.; Wang, Y.; Christie, A. L.; West, N.; Cameron, M. J.; Schwartz, B.; Heightman, T. D.; La Thangue, N.;

French, C. A.; Wiest, O.; Kung, A. L.; Knapp, S.; Bradner, J. E. Selective Inhibition of BET Bromodomains. *Nature* **2010,** 468, 1067-1073.

22.   Chung, C. W.; Coste, H.; White, J. H.; Mirguet, O.; Wilde, J.; Gosmini, R. L.; Delves, C.; Magny, S. M.; Woodward, R.; Hughes, S. A.; Boursier, E. V.; Flynn, H.; Bouillot, A. M.; Bamborough, P.; Brusq, J. M.; Gellibert, F. J.; Jones, E. J.; Riou, A. M.; Homes, P.; Martin, S. L.; Uings, I. J.; Toum, J.; Clement, C. A.; Boullay, A. B.; Grimley, R. L.; Blandel, F. M.; Prinjha, R. K.; Lee, K.; Kirilovsky, J.; Nicodeme, E. Discovery and Characterization of Small Molecule Inhibitors of the BET Family Bromodomains. *J. Med. Chem.* **2011,** 54, 3827-3838.

23.   Picaud, S.; Wells, C.; Felletar, I.; Brotherton, D.; Martin, S.; Savitsky, P.; Diez-Dacal, B.; Philpott, M.; Bountra, C.; Lingard, H.; Fedorov, O.; Muller, S.; Brennan, P. E.; Knapp, S.; Filippakopoulos, P. RVX-208, an Inhibitor of BET Transcriptional Regulators with Selectivity for the Second Bromodomain. *Proc. Natl. Acad. Sci. U. S. A.* **2013,** 110, 19754-19759.

24.   Resverlogix announces topline results in BETonMACE phase 3 epigenetics trial. https://www.resverlogix.com/investors/news?article=647 (accessed Sep 30, 2019).

25.   McDaniel, K. F.; Wang, L.; Soltwedel, T.; Fidanze, S. D.; Hasvold, L. A.; Liu, D.; Mantei, R. A.; Pratt, J. K.; Sheppard, G. S.; Bui, M. H.; Faivre, E. J.; Huang, X.; Li, L.; Lin, X.; Wang, R.; Warder, S. E.; Wilcox, D.; Albert, D. H.; Magoc, T. J.; Rajaraman, G.; Park, C. H.; Hutchins, C. W.; Shen, J. J.; Edalji, R. P.; Sun, C. C.; Martin, R.; Gao, W.; Wong, S.; Fang, G.; Elmore, S. W.; Shen, Y.; Kati, W. M. Discovery of N-(4-(2,4-Difluorophenoxy)-3-(6-methyl-7-oxo-6,7-dihydro-1H-pyrrolo[2,3-c]pyridin-4-yl)phenyl)ethanesulfonamide   (ABBV-075/Mivebresib), a Potent and Orally Available Bromodomain and Extraterminal Domain (BET) Family Bromodomain Inhibitor. *J. Med. Chem.* **2017,** 60, 8369-8384.

26.   Gavai, A. V.; Norris, D.; Tortolani, D.; Malley, D.; Zhao, Y.; Quesnelle, C.; Gill, P.; Vaccaro, W.; Huynh, T.; Ahuja, V.; Dodd, D.; Mussari, C.; Harikrishnan, L.; Kamau, M.; Tokarski, J. S.; Sheriff, S.; Rampulla, R.; Wu, D.-R.; Li, J.; Zhang, H.; Li, P.; Sun, D.; Yip, H.; Zhang, Y.; Mathur, A.; Zhang, H.; Huang, C.; Yang, Z.; Ranasinghe, A.; Arienzo, C.; Su, C.; Everlof, G.; Zhang, L.; Raghavan, N.; Hunt, J. T.; Poss, M.; Vite, G. D.; Westhouse, R. A.; Wee, S. Abstract 5789: Discovery of Clinical Candidate BMS-986158, an Oral BET Inhibitor, for the Treatment of Cancer. *Cancer Res.* **2018,** 78, 5789.

27.   Raux, B.; Voitovich, Y.; Derviaux, C.; Lugari, A.; Rebuffet, E.; Milhas, S.; Priet, S.; Roux, T.; Trinquet, E.; Guillemot, J. C.; Knapp, S.; Brunel, J. M.; Fedorov, A. Y.; Collette, Y.; Roche, P.; Betzi, S.; Combes, S.; Morelli, X. Exploring Selective Inhibition of the First Bromodomain of the Human Bromodomain and Extra-terminal Domain (BET) Proteins. *J. Med. Chem.* **2016,** 59, 1634-1641.

28.   Tian, X.; Song, L.; Li, E.; Wang, Q.; Yu, W.; Chang, J. Metal-Free One-Pot Synthesis of 1,3-Diazaheterocyclic Compounds via I2-Mediated Oxidative C–N Bond Formation. *RSC Adv.* **2015,** 5, 62194-62201.

29.   Pettersson, M.; Hou, X.; Kuhn, M.; Wager, T. T.; Kauffman, G. W.; Verhoest, P. R. Quantitative Assessment of the Impact of Fluorine Substitution on P-Glycoprotein (P-gp) Mediated Efflux, Permeability, Lipophilicity, and Metabolic Stability. *J. Med. Chem.* **2016,** 59, 5284-5296.

30.   Battye, T. G.; Kontogiannis, L.; Johnson, O.; Powell, H. R.; Leslie, A. G. iMOSFLM: a New Graphical Interface for Diffraction-Image Processing with MOSFLM. *Acta Crystallogr. D Biol. Crystallogr.* **2011,** 67, 271-281.

31.   Evans, P. R.; Murshudov, G. N. How Good Are My Data and What is the Resolution? *Acta Crystallogr. D Biol. Crystallogr.* **2013,** 69, 1204-1214.

32.   Adams, P. D.; Afonine, P. V.; Bunkoczi, G.; Chen, V. B.; Davis, I. W.; Echols, N.; Headd, J. J.; Hung, L. W.; Kapral, G. J.; Grosse-Kunstleve, R. W.; McCoy, A. J.; Moriarty, N. W.; Oeffner, R.; Read, R. J.; Richardson, D. C.; Richardson, J. S.; Terwilliger, T. C.; Zwart, P. H. PHENIX: a Comprehensive Python-Based System for Macromolecular Structure Solution. *Acta Crystallogr. D Biol. Crystallogr.* **2010,** 66, 213-221.

33.   Emsley, P.; Lohkamp, B.; Scott, W. G.; Cowtan, K. Features and Development of Coot. *Acta Crystallogr. D Biol. Crystallogr.* **2010,** 66, 486-501.

34.   Ding, C.; Zhang, Y.; Chen, H.; Yang, Z.; Wild, C.; Chu, L.; Liu, H.; Shen, Q.; Zhou, J. Novel Nitrogen-Enriched Oridonin Analogues with Thiazole-Fused A-Ring: Protecting Group-Free Synthesis, Enhanced Anticancer Profile, and Improved Aqueous Solubility. *J. Med. Chem.* **2013,** 56, 5048-5058.

35.   Chen, H.; Yang, Z.; Ding, C.; Chu, L.; Zhang, Y.; Terry, K.; Liu, H.; Shen, Q.; Zhou, J. Discovery of O-Alkylamino Tethered Niclosamide Derivatives as Potent and Orally Bioavailable Anticancer Agents. *ACS Med. Chem. Lett.* **2013,** 4, 180-185.

36.   Kiselev, E.; DeGuire, S.; Morrell, A.; Agama, K.; Dexheimer, T. S.; Pommier, Y.; Cushman, M. 7-Azaindenoisoquinolines as Topoisomerase I Inhibitors and Potential Anticancer Agents. *J. Med. Chem.* **2011,** 54, 6106-6116.

37.   Tian, B.; Li, X.; Kalita, M.; Widen, S. G.; Yang, J.; Bhavnani, S. K.; Dang, B.; Kudlicki, A.; Sinha, M.; Kong, F.; Wood, T. G.; Luxon, B. A.; Brasier, A. R. Analysis of the TGFbeta-Induced Program in Primary Airway Epithelial Cells Shows Essential Role of NF-kappaB/RelA Signaling Network in Type II Epithelial Mesenchymal Transition. *BMC Genomics* **2015,** 16, 529.

38.   Tian, B.; Zhao, Y.; Sun, H.; Zhang, Y.; Yang, J.; Brasier, A. R. BRD4 Mediates NF-kappaB-Dependent Epithelial-Mesenchymal Transition and Pulmonary Fibrosis via Transcriptional Elongation. *Am. J. Physiol. Lung Cell Mol. Physiol.* **2016,** 311, L1183-L1201.

39.   Tian, B.; Zhao, Y.; Kalita, M.; Edeh, C. B.; Paessler, S.; Casola, A.; Teng, M. N.; Garofalo, R. P.; Brasier, A. R. CDK9-Dependent Transcriptional Elongation in the Innate Interferon-Stimulated Gene Response to Respiratory Syncytial Virus Infection in Airway Epithelial Cells. *J. Virol.* **2013,** 87, 7075-7092.

Table of Contents (TOC) Graphic

45 (ZL0516)

BRD4 BD1 IC_{50} = 84 nM
BRD4 BD2 IC_{50} = 718 nM
F = 35%
aqueous solubility > 50 mg/mL
hERG IC_{50} > 30 μM
No obvious CYP450 inhibition

BRD4_BD1:ZL0516